

TOPICAL REVIEW

## Recent advances in high-throughput superconductivity research

To cite this article: Jie Yuan *et al* 2019 *Supercond. Sci. Technol.* **32** 123001

View the [article online](#) for updates and enhancements.




**IOP | ebooks™**

Bringing you innovative digital publishing with leading voices to create your essential collection of books in STEM research.

Start exploring the collection - download the first chapter of every title for free.

## Topical Review

# Recent advances in high-throughput superconductivity research

Jie Yuan<sup>1,2</sup>, Valentin Stanev<sup>3</sup>, Chen Gao<sup>4</sup>, Ichiro Takeuchi<sup>3</sup> and Kui Jin<sup>1,2,5</sup> 

<sup>1</sup> Beijing National Laboratory for Condensed Matter Physics, Institute of Physics, Chinese Academy of Sciences, Beijing 100190, People's Republic of China

<sup>2</sup> Key Laboratory of Vacuum Physics, School of Physical Sciences, University of Chinese Academy of Sciences, Beijing 100049, People's Republic of China

<sup>3</sup> Department of Materials Science and Engineering, University of Maryland, College Park, Maryland 20742, United States of America

<sup>4</sup> Beijing Advanced Sciences and Innovation Center of Chinese Academy of Sciences, Beijing 101407, People's Republic of China

<sup>5</sup> Songshan Lake Materials Laboratory, Dongguan, Guangdong 523808, People's Republic of China

E-mail: [yuanjie@iphy.ac.cn](mailto:yuanjie@iphy.ac.cn), [takeuchi@umd.edu](mailto:takeuchi@umd.edu) and [kuijin@iphy.ac.cn](mailto:kuijin@iphy.ac.cn)

Received 12 October 2018, revised 7 October 2019

Accepted for publication 28 October 2019

Published 13 November 2019



CrossMark

## Abstract

Applications are being found for superconducting materials in a rapidly growing number of technological areas, and the search for novel superconductors remains a major scientific task. However, the steady increase in the complexity of candidate materials presents a big challenge to researchers. In particular, conventional experimental methods are not well suited to an efficient search for candidates in a compositional space growing exponentially with the number of elements; neither do they permit a quick extraction of reliable multidimensional phase diagrams delineating the physical parameters that control superconductivity. New research paradigms that can boost the speed and the efficiency of research into superconducting materials are urgently needed. High-throughput methods for the rapid screening and optimization of materials have aided the acceleration of research in bioinformatics and the pharmaceutical industry, yet remain rare in quantum materials research. In this paper we briefly review the history of high-throughput research and then focus on some recent applications of this paradigm in superconductivity research. We consider the role these methods can play in all stages of materials development, including high-throughput computation, synthesis, characterization, and the emerging field of machine learning for materials. The high-throughput paradigm will undoubtedly become an indispensable tool in superconductivity research in the near future.

Keywords: superconductivity, high-throughput, machine learning, combinatorial film, rapid screening

(Some figures may appear in colour only in the online journal)

## 1. Introduction

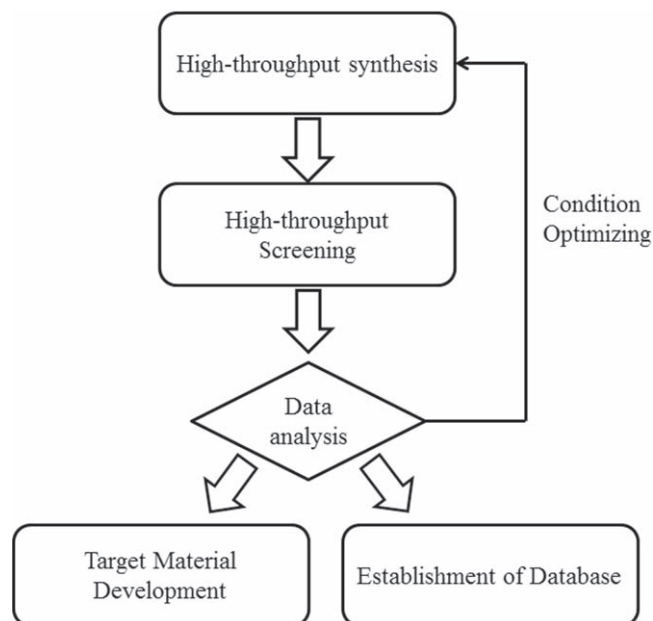
Ever since 1911, when Kammerlingh Onnes in Leiden observed the disappearance of the electrical resistance of mercury at very low temperatures, the phenomenon of

superconductivity has been intensely studied. Yet the exact nature of this effect remained unclear until the Bardeen–Cooper–Schrieffer (BCS) theory was developed in 1957 [1, 2]. Establishing the physical parameters behind the critical temperature ( $T_c$ ) then became one of the main research topics

in the field. The observation of an isotope effect clearly demonstrated that  $T_c$  in most of the superconductors known at the time was linked to the coupling between the electrons and the lattice, with the strength of the electron-phonon (el-ph) interaction playing a key role. Increasing el-ph coupling enhances  $T_c$  provided the atoms in the crystal vibrate near their equilibrium sites only. But as the coupling strength crosses from a weak regime to an intermediate regime, the normal metallic state itself becomes unstable and a competing state such as a charge density wave may arise, causing structural changes. Although early analyses pointing to a ceiling of  $T_c$  at about 30–40 K proved too simplistic, it quickly became clear that achieving significantly higher critical temperatures would require unusual conditions or materials [3]. (One example is the recent remarkable observation of high  $T_c$  in hydrogen-rich materials under extreme pressure [4]).

In 1986, the ceramic compound Ba-La-Cu-O was found to become superconducting at 35 K by Bednorz and Müller in Zurich [5]. This milestone work not only raised hopes for superconductors with a  $T_c$  above 40 K, but also inspired other physicists to expand their search by exploring compounds with complex crystal structures and containing multiple elements. Soon, the limit of 40 K was crossed [6, 7]; critical temperatures above that of liquid nitrogen (77 K) were realized [8, 9], and the highest  $T_c$  of 138 K was reached in the case of  $\text{Hg}_{0.8}\text{Tl}_{0.2}\text{Ba}_2\text{Ca}_2\text{Cu}_3\text{O}_{8.33}$  (at ambient pressure) [10]. While these discoveries inspired a generation of researchers, the mechanism of superconductivity in this class of materials (dubbed cuprates) is still a mystery.

Before the discovery of high- $T_c$  cuprate (HTSCs) materials, most known superconductors were composed of no more than two elements and were predominantly elemental superconductors, alloys, and intermetallics. As the highest superconducting transition temperature passed 40 K, the superconducting compounds became more complex and contained more elements; for example,  $\text{YBa}_2\text{Cu}_3\text{O}_{6+\delta}$ ,  $\text{HgBa}_2\text{Ca}_2\text{Cu}_3\text{O}_{8+\delta}$  and  $\text{Hg}_{0.8}\text{Tl}_{0.2}\text{Ba}_2\text{Ca}_2\text{Cu}_3\text{O}_{8.33}$  are comprised of four, five, and six elements respectively. On the other hand, the recent discoveries of Fe-based [11, 12], Cr-based and Mn-based [13–15] superconductors demonstrated that even compounds with elements once thought strongly detrimental to superconductivity must be considered. Obviously, the number of possible combinations grows exponentially as more and more elements are added to the list of candidate materials. The number of compounds can be easily estimated within the group of natural elements; the order of magnitudes for possible combinations are  $10^3$ ,  $10^5$ ,  $10^7$  and  $10^9$  for binary, ternary, quaternary, and pentenary compounds, respectively. In addition, many other methods of modulating superconductivity are known: ultra-high pressure [16, 17], ultra-thin film deposition [18], superlattice architecture [19] and ionic liquid/solid gating [20, 21] are examples. Further, some HTSC materials are extremely sensitive to physical and chemical parameters. For instance, a one percent variation in cation content can turn a copper oxide superconductor into an insulator [22]. A vast amount of synthesis is then required, to construct a reliable and detailed phase



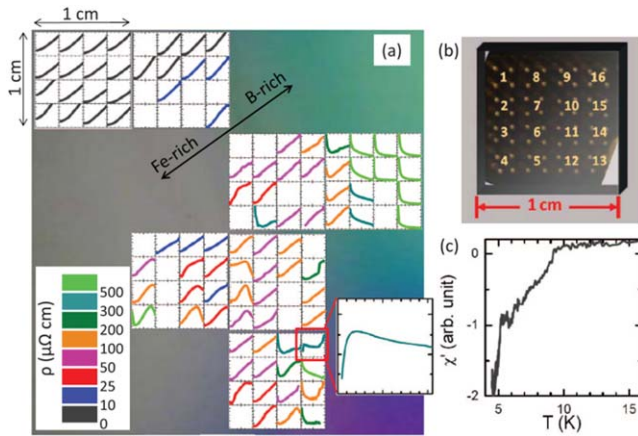
**Figure 1.** The high-throughput approach for discovery and development of materials.

diagram as a function of cation and anion contents [23]. What is more, a complete phase diagram of HTSC must necessarily be multivariate; i.e., alongside cation and anion substitutions it must include synthesis conditions, pressure, magnetic field, and other variables. It is clearly not feasible to efficiently construct such a multidimensional phase diagram using the traditional one-material-at-a-time experimental methodology.

In general, there are two main challenges in the experimental study of superconductivity: i) searching for novel superconductors from among the enormous number of candidate compounds comprised of more and more elements, and; ii) delineating the key physical parameters that control the superconductivity, by means of establishing a reliable multidimensional phase diagram. Conventional experimental methods are not well suited to addressing these problems, and new paradigms and tools are required to improve the efficiency of superconductivity research [24, 25].

In bioinformatics and in the pharmaceutical industry, similar challenges arose before the discovery of HTSCs. There is a huge number of possible gene combinations and drug formulas, and it is not realistic to synthesize and test them one by one. The idea of carrying out many tests simultaneously—the so-called high-throughput strategy—was rapidly developed and put into practice. Ever since, high-throughput methods have been a driving force behind the development of modern biology and medicine. This methodology was also gradually adopted in condensed matter physics and materials science.

The general high-throughput materials research procedure has the following steps: sample synthesis, characterization, and analysis of the data. Any significant increase in efficiency necessitates the acceleration of every step, as well as substantial coordination among them. The high-throughput approach for materials development is sketched in figure 1.



**Figure 2.** Mapping of the temperature dependence of resistivity on the Fe-B composition spread film. Reprinted from [36], with the permission of AIP Publishing.

In 1970, Hanak introduced the rudiments of a multiple sample concept in materials research by developing a multiple-target, radio-frequency co-sputtering deposition [26]. However, the difficulties in obtaining and processing a large amount of experimental data prevented the widespread adoption of high-throughput methods in materials research at the time. Another factor inhibiting the spread of these methods was the low demand for complex functional materials. This has dramatically changed in recent decades, owing to the needs of industries such as communications, aerospace, energy, and transportation. The demand for novel materials has undergone explosive growth, in terms of both diversity and required performance. This necessitated significant acceleration of materials research and development. High-throughput synthesis and characterization technology became a major research tool, leading to substantial progress in a number of applications (see, for example, 27–34). The rapid progress in information technologies aided these advances by creating powerful tools able to deal with the massive amounts of data generated by this approach.

Thus, the high-throughput method is an extremely promising approach with which to meet the challenges in superconductivity research outlined above. In one early pioneering work demonstrating the potential of these methods, Xiang *et al* reported the rapid synthesis of high- $T_c$  superconductors, with 128 copper oxide superconducting thin films deposited on a single substrate in one batch [35]. Although the superconductors synthesized in this work were already known, the increase in efficiency achieved by the parallel synthesis was encouraging. In 2013, Jin *et al* provided the first example of a superconductor discovered via the high-throughput methodology. They fabricated composition-spread films comprised of Fe and B across three-inch Si wafers by a co-sputtering technique. Indications of a superconducting region were found from the resistance measurement, carried out with a home-made probe with an array of 64 pogo-pins (figure 2(b)). Superconductivity was then confirmed by a zoom-in magnetotransport and susceptibility measurements [36]. In 2016, Wu *et al* studied a collection of heterostructures comprised of  $\text{La}_2\text{CuO}_4$  and combinatorial  $\text{La}_{2-x}\text{Sr}_x\text{CuO}_4$

( $0.15 \leq x \leq 0.47$ ), achieved by varying the deposition rate of the Sr content in an advanced oxide molecular beam epitaxy system [37]. In 2018, Stanev *et al* filtered more than 100,000 compounds and created a list of potential superconductors, using a machine learning model trained on the critical temperatures of more than 12,000 known superconductors [38].

As seen from these examples, the high-throughput paradigm is already starting to permeate superconductivity research. In this review we outline the advances made in all parts of high-throughput superconductivity research: high-throughput synthesis (section 2), high-throughput characterizations (section 3), high-throughput *ab initio* calculations (section 4), and machine learning (section 5). We also discuss the necessity to develop the next generation of facilities, techniques, and platforms in order to make full use of high-throughput methods (discussed in section 6) [36].

## 2. High-throughput syntheses for superconductors

High-throughput synthesis is one of the foundations of the recent acceleration of the rate of materials exploration. However, that does not mean that the cost of synthesis has suddenly become irrelevant. Efficiency is a key point; the speed of synthesis should increase faster than the resources it demands. To achieve this, common components and procedures used at different experimental steps, such as evacuation, heating, and conditioning atmosphere, should be combined as much as possible. This is the basis of the so-called combinatorial approach, which is the most efficient high-throughput synthesis method. Koinuma *et al* published the basic concept of combinatorial chemistry for solid state materials in [39]. During synthesis, a chemical reaction for the target material is influenced by many factors. The search for new materials can be regarded as a process of scanning certain points in the phase diagram as a function of multiple variables, as shown in figure 3. Compared to the classical synthesis process of an effective point-by-point search, a combinatorial approach can much more quickly map the key parameters (such as composition, temperature, and pressure) responsible for optimizing a functionality.

Thin-film preparation technology is the most widely used combinatorial synthesis method [30]. As early as 1965, Kennedy *et al* reported a method for rapidly obtaining a Fe-Cr-Ni ternary library by electron beam co-evaporation of three precursors (Fe, Cr, and Ni targets), on an equilateral triangle of metal foil with a side length of 10 inches [41]. Three generations of combinatorial film growth techniques have been developed since then. The first generation realized a gradient chemical composition by ablating the precursors simultaneously and mixing them using natural diffusion. Co-evaporation [41, 42], co-sputtering [26, 43, 40], and co-laser ablating [44] techniques are all categorized into this generation. Figure 4 shows a typical configuration of a co-sputtering system. Different sources are mounted against the wafer at a certain angle to the normal direction of the wafer surface. During the deposition, such a configuration results in a spatial variation of the deposition rate and allows plumes from different targets to overlap and form a natural composition

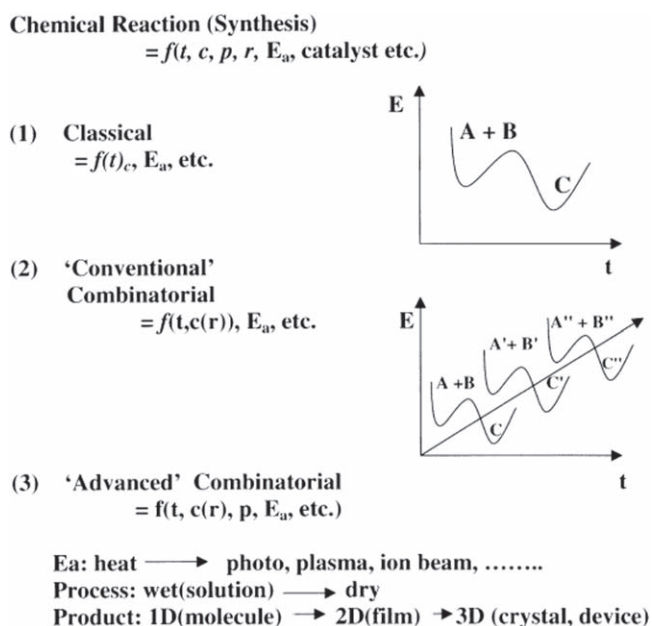


**Figure 3.** Concepts of combinatorial synthesis versus classical synthesis. Reprinted from [40], Copyright (1998), with permission from Elsevier.

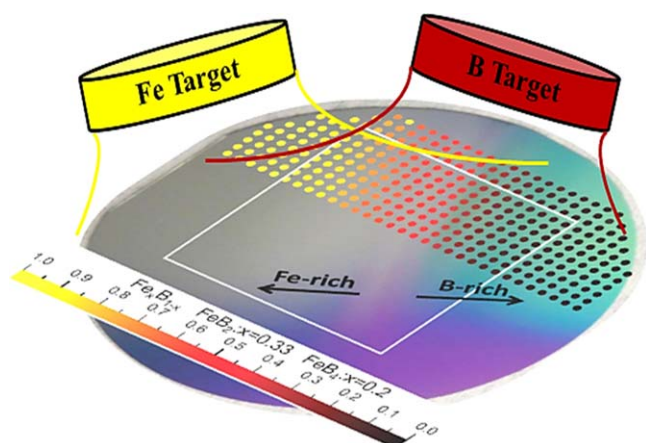


**Figure 4.** Sketch of the co-sputtering deposition for an Fe-B composition spread combi-film. Reprinted from [36], with the permission of AIP Publishing.

gradient. Recently, Jin *et al* obtained an Fe-B binary spread by such a method, with a continuous composition across a three-inch Si wafer with a 200 nm SiO<sub>2</sub> layer on top [36]. The lower part of figure 4 shows a photograph of a composition spread wafer taken under natural light; the average composition at different positions (solid circles) is obtained by wavelength dispersive spectroscopy (WDS). A key advantage of the co-deposition method is that it requires relatively simple facilities and the deposition process is easy to control. However, the chemical composition cannot be precisely controlled because of the natural variability of the spatial deposition rate. The local composition of the film can only be determined by micro-region analysis methods (as discussed in the section on high-throughput characterizations).

Second-generation methods were developed to overcome the shortcomings of the co-deposition approach. Xiang *et al*

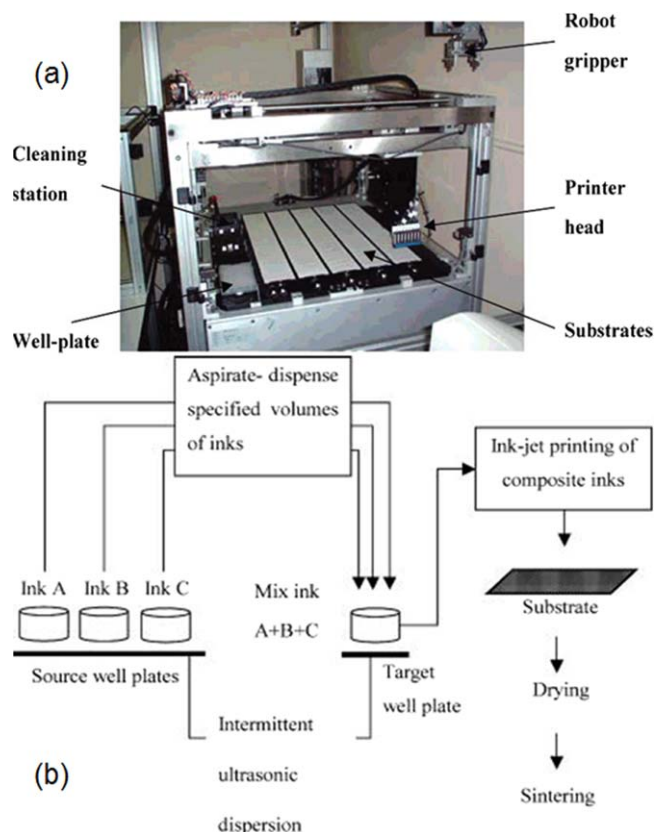


**Figure 5.** (a) The ink-jet printer table within the robot gantry, populated with alumina substrates. The 'pick and place' robot arm is seen at the top right. (b) Schematic diagram of the mixing and printing protocol. Reprinted with permission from [48]. Copyright (2005) American Chemical Society.

used a method combining thin film deposition and physical mask techniques for a parallel synthesis of spatially addressable libraries of materials [35]. The programmable mask is at the core of the second-generation technology. Films fabricated using these methods contain discrete squares with varying compositions. Because these small regions are addressable, such films are also called integrated materials chips or combinatorial materials libraries. More details about this synthesis method can be found in the earlier literature (e.g., in 32, 45–47). It must be noted that the mask is not necessarily a physical one. Wang *et al* developed a combinatorial robot able to create thick-film libraries by ink-jet printing, as shown in figure 5 [48]. After being ground into sufficiently fine powder, precursors can be made into inks [49], taking the role of the three 'primary colors'. Different doses of inks are ejected on designated places on the wafer. Thus, using selected precursors and an appropriate post-processing, an addressable materials library can be created. In this way, the ejector together with the robot arm replaces the physical mask [50, 51].

Mask patterns have been widely used in the study of electronic, magnetic, optical and dielectric materials, as well as catalysts and alloys [52]. However, for more precise studies of material properties, distinct techniques are required, such as atomically controlled layer-by-layer thin-film growth [25].

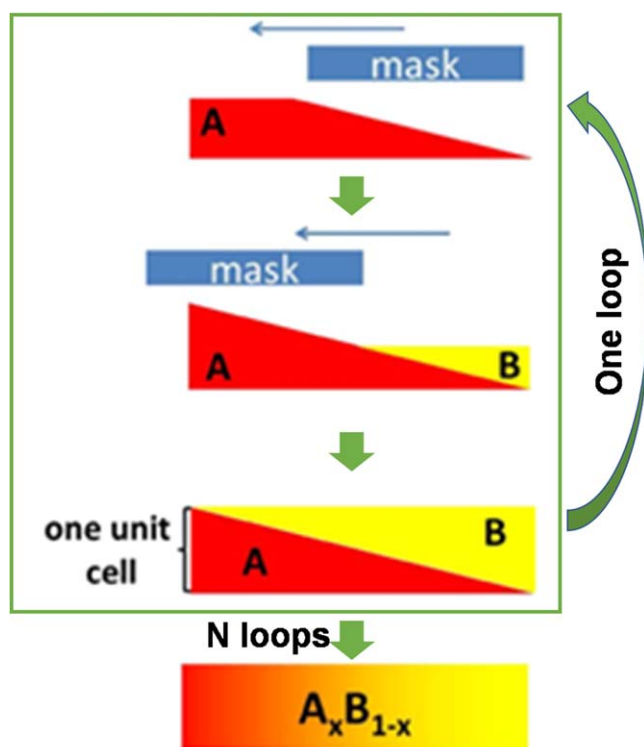


**Figure 6.** Schematic of binary combinatorial film growth using the continuous moving mask technique. Reprinted by permission from Springer Nature Customer Service Centre GmbH: Springer Nature, Science China Physics, Mechanics and Astronomy, [54], 2017.

Combinatorial laser molecular beam epitaxy (CLMBE)—the so-called third generation of combinatorial thin-film preparation technology—was developed to carry out parallel fabrication via a layer-by-layer growth mode [25]. The state-of-the-art laser molecular beam epitaxy in combination with a mobile mask technique has already been used to control layering sequences of high-quality superconducting films [53]. The procedure for preparing binary combinatorial films with a continuous chemical composition spread on a single substrate can be briefly described as follows (see also figure 6). Once a target A is ablated by laser pulses, a metal mask is moved along the substrate in half a period of time and results in a linear distribution of the A component. In the other half-period, target B is ablated for a reverse distribution by moving the mask in the opposite direction [54]. The desired thickness of the combinatorial film can be achieved by setting corresponding periods of deposition. It should be emphasized that the two precursors A and B must be mixed in a single unit cell in the time period, monitored by the reflection high-energy electron diffraction system for *in situ* diagnostics. Otherwise, a superlattice will be obtained rather than a combinatorial film.

CLMBE is easy to operate, and benefits from a wide chemical composition range in one batch of deposition. This makes it perfect for obtaining precise phase diagrams of materials such as cuprate superconductors [5]. For instance, Yu *et al* fabricated a combinatorial  $\text{La}_{2-x}\text{Ce}_x\text{CuO}_{4\pm\delta}$  thin film with values of  $x$  from 0.1 to 0.19 on a  $1 \times 1 \text{ cm}^2$   $\text{SrTiO}_3$  substrate by CLMBE [54].

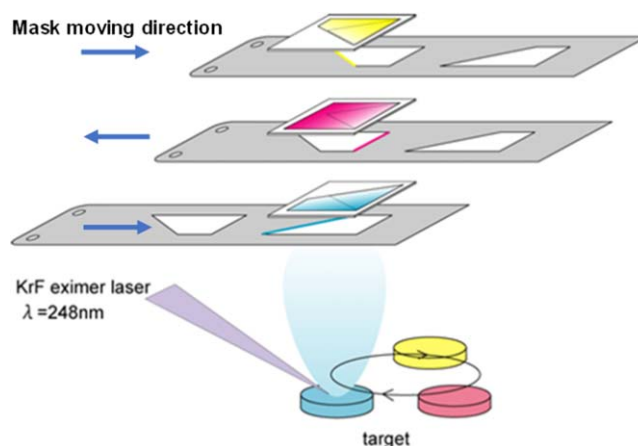


**Figure 7.** (From the introduction brochure of Pascal Co., Ltd of Japan.) Schematic of ternary combinatorial film growth using the continuous moving mask technique. The blue arrows indicate the direction of mask motion at each step.

Following the same principle, a ternary combinatorial film can be grown by ablating three targets alternately and shadowing the substrate from three directions by mask with a sophisticated pattern design (shown in figure 7). With this method, Mao *et al* prepared an Mg–Ni–Al ternary thin film library [24]. In combinatorial films, the chemical composition is locked to the fixed space point of the sample surface. For a ternary compound, the formula can be written as  $\text{A}_x\text{B}_y\text{C}_{1-x-y}$ , in which A, B, and C are different elements. Since there are two independent spatial coordinators (e.g.,  $x$  and  $y$ ) determining the position corresponding to a unique chemical composition, the full ternary library can be obtained based on a single combinatorial spread. However, if more than two variables are involved, e.g., three variables in the quaternary  $\text{A}_x\text{B}_y\text{C}_z\text{D}_{1-x-y-z}$ , one cannot obtain all the combinations of these four components in a single chip; instead, a pseudo multi-component materials library can be created.

As explained above, three generations of distinct combinatorial film preparation techniques have been developed. It must be noted that each generation has its own unique merits, and is suitable for different kinds of materials. Sometimes a customized combinatorial approach is required, for example for compounds that show superconductivity only in a very narrow range of chemical doping. A typical iron-based superconductor,  $\text{FeSe}_{1-\delta}$ , displays superconductivity only within a finite  $\delta$  [55]. Since Se is a volatile element, fine control of the Fe/Se ratio of the final film can be extremely challenging using the methods presented above. Recently, a double-beam laser configuration was used to produce a redistributed laser flux density on a FeSe target. As reported in the study of  $\text{SrTiO}_3$  films grown by pulsed laser deposition (PLD), the stoichiometric ratio can be regulated by the power density of the laser [56]. Tuning the parameter of the combinatorial laser, the Fe/Se ratio of the final film can be varied by a very narrow  $\delta$  step (i.e., the order of magnitude is  $\sim 0.001$ , which is beyond the resolution limit of the common chemical analysis methods). The left panel of figure 8 is a schematic of the double-beam laser used in the deposition; the corresponding evolution of the superconducting

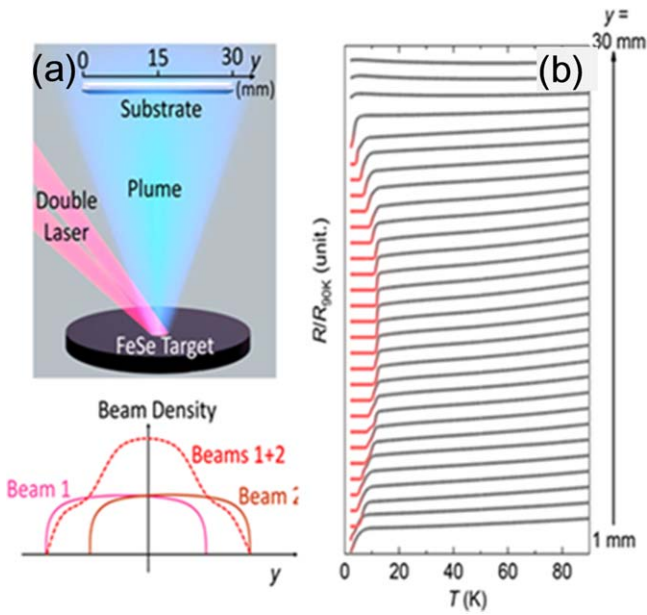


**Figure 8.** (a) Schematic process of the double-beam pulsed laser deposition via spectroscopy, and then focused onto the target with controllable displacement. (b) The temperature dependence of normalized resistance along the  $y$  direction, with the highest  $T_c$  in the middle. Reproduced with permission from [57].

critical temperature can be clearly seen in the normalized  $R$ - $T$  curves from different space regions of the final film (right panel). Moving along the film from one edge to the other,  $T_c$  changes continuously from below 2 K to 12 K and back to below 2 K. There is no obvious difference in the film thickness ( $\sim 150$  nm) across the whole film (verified by scanning electron microscope (SEM)); thus, any thickness influence on  $T_c$  can be excluded. Such combinatorial films offer a good platform to investigate the nature of tunable superconductivity in the Fe-Se binary system [57].

Wu *et al* used a tilted Knudsen cell in an oxide molecular beam epitaxy system to synthesize a combinatorial  $\text{La}_{2-x}\text{Sr}_x\text{CuO}_4$  film. Although in principle this falls into the class of first-generation combinatorial techniques, it provides much finer control over the composition. The deposition rate can be precisely tuned and the growth process can be monitored *in situ*. The composition gradient originates in the angle between the sources and the substrate, as shown in figure 9. By means of this method, the composition across the film can be confined to extremely fine steps,  $\Delta x \sim 0.00008$  [37, 58].

In addition to generating composition-spread material libraries, combinatorial approaches can be used to rapidly ascertain the optimal growth condition for superconducting materials. For example, the conventional way to find the best deposition temperature of a superconducting material is to try temperatures one by one. However, a much more efficient method is to create a thermal gradient on the substrate during film deposition [59]. Figure 10 shows one configuration which can create such a gradient during the growth process. One end of the substrate is attached to a heater while the other end is kept free-standing. When the heater is set at high temperature, heat diffuses to the free-standing end through the substrate. Using such a

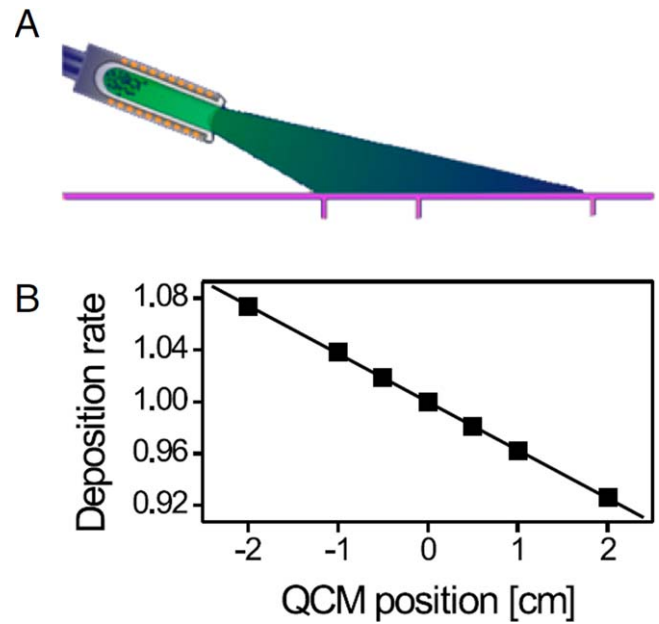


**Figure 9.** Schematics of the deposition geometry: a thermal effusion cell is positioned at a shallow angle ( $20^\circ$ ) with respect to the substrate. Closer to the source, the deposition rate is higher. Reproduced with permission from [37]. PNAS April 19, 2016 113 (16) 4284-4289.

configuration, a temperature range was found in which only a pure  $\beta$ -FeSe phase forms. Only three batches of samples were tested, with deposition temperatures from  $350^\circ\text{C}$  to  $700^\circ\text{C}$  [60].

In addition, parallel synthesis can help to reduce the uncertainty originating in the difference between growth conditions, which is unavoidable between separate experimental batches. Figure 11 shows the relationship between the out-of-plane crystal lattice parameter ( $c$ -axis) and  $T_c$  extracted from more than 1 000 pieces of uniform FeSe films (upper panel) as well as one combinatorial film (lower panel), respectively. It took almost three years to prepare and characterize the 1 000 + uniform films; this is in contrast with the several weeks needed for the single combinatorial film. As can be seen, the amount of data collected from the uniform films is much larger. However, the positive relation between  $c$  and  $T_{c0}$  is manifested much more clearly in the combinatorial film data.

Combinatorial film data provides a better correlation between  $T_c$  and lattice parameters due to its more precise composition control.

### 3. High-throughput characterizations of superconductors

As another step in the high-throughput methodology, rapid characterization of combinatorial films is indispensable in the drive to accelerate superconductivity research. By the nature of combinatorial synthesis, characterization has to be conducted by probes with spatial resolution capabilities. Several commercially available probes satisfy this requirement: the atomic force microscope, scanning tunneling microscope (STM), optical microscope, and scanning electron microscope

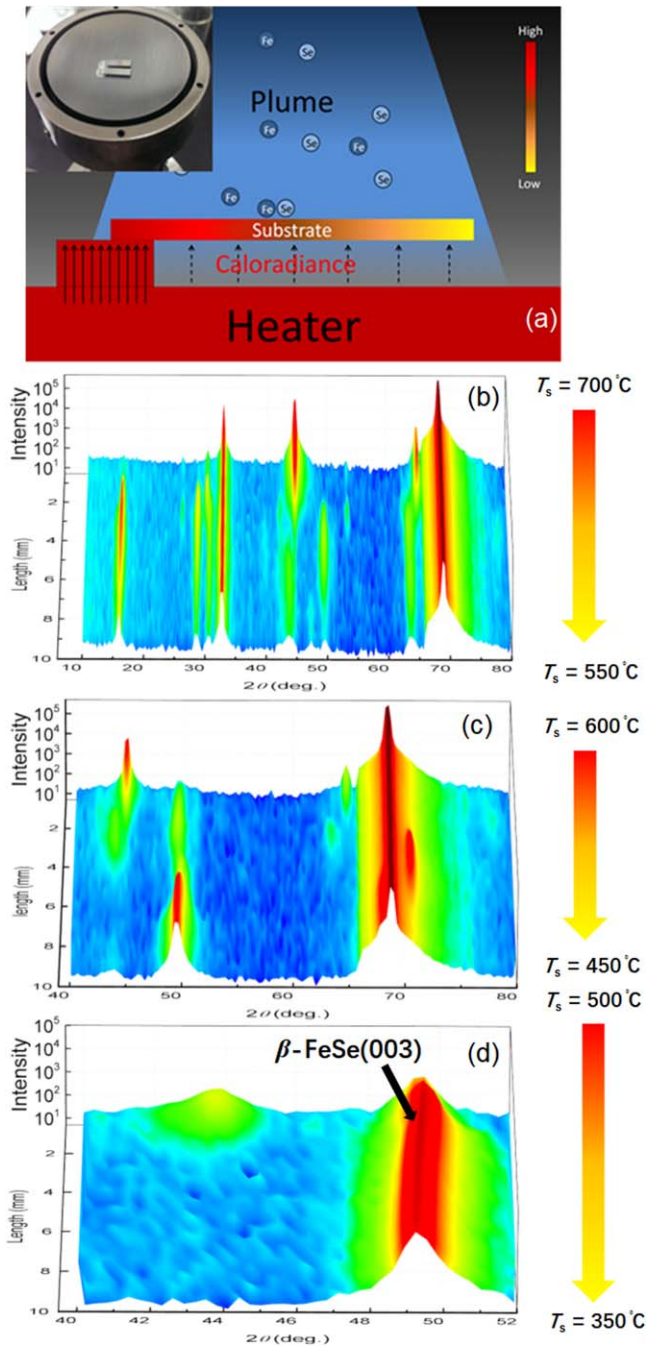


**Figure 10.** (a) Schematic of combinatorial film growth with gradient temperature, inset on top left is a real photo of the substrate mounted on the heater. (b)–(d) The micro-region  $\theta/2\theta$  x-ray patterns of the FeSe films grown using different temperature gradients: 700 °C to 550 °C; 600 °C to 450 °C, and 500 °C to 350 °C, respectively. A pure  $\beta$ -FeSe phase can be found in the region where the deposition temperature is not beyond 450 °C [60].

are just a few examples. Such items of equipment, with an auto-scan functionality, can have high spatial resolution, and are equipped with tips or aggregated beams. There are also diverse homemade probes designed to study various properties of high-throughput samples. In this section we consider techniques relevant to superconductivity research, briefly summarized in the following order.

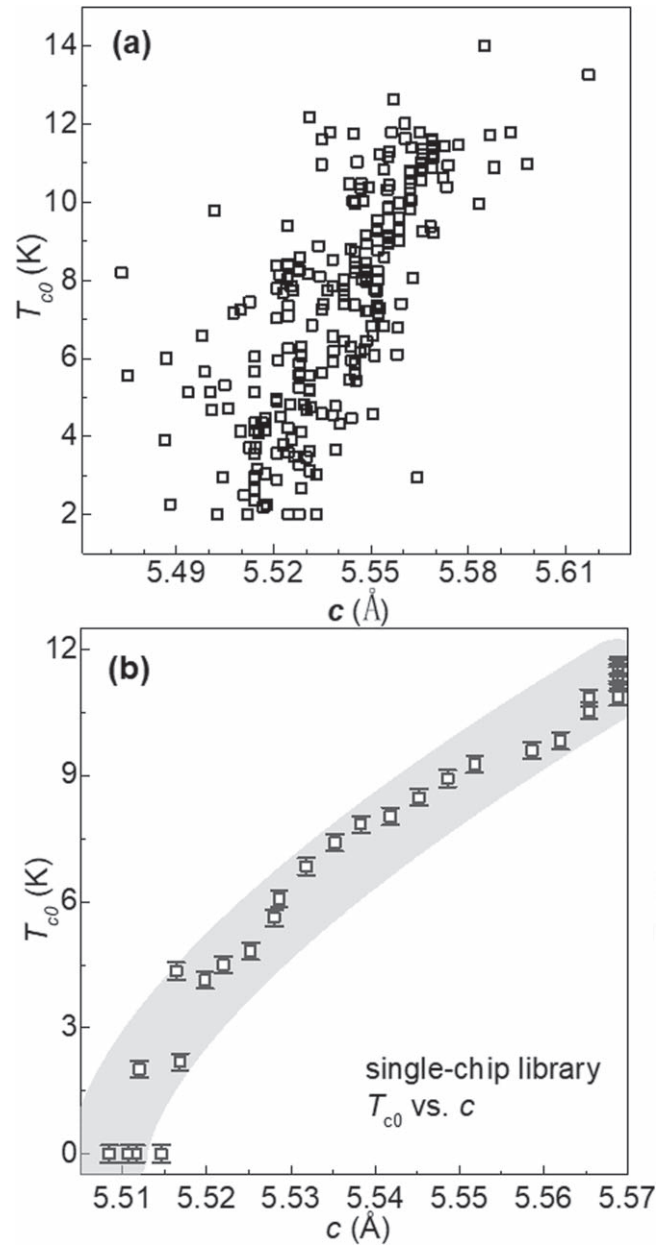


**Figure 11.** The  $c$ -axis lattice constants' dependence on  $T_{c0}$  for (a) uniform FeSe films, (b) combinatorial FeSe film with gradient  $T_c$ . Reproduced with permission from [57].

### 3.1. Composition and structure

Probes commonly used for composition and structure analyses are: x-ray diffraction; scanning electron microscopy (SEM); and transmission electron microscopy (TEM). Because the electron beam can be focused, methods using it naturally provide the required spatial resolution and can be used for high-throughput characterizations [33, 61].

Great efforts have been made to develop spatially resolved x-ray-based characterization methods. Since x-rays have much higher frequency and photon energy than visible light, they tend to penetrate or become absorbed in most materials. Unfortunately, most of the techniques used to redirect x-rays are unable to produce well focused beams.



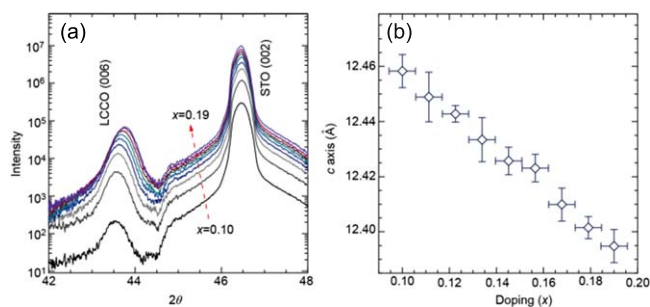


**Figure 12.** (a) The micro-region x-ray diffraction results of combi-film  $\text{La}_{2-x}\text{Ce}_x\text{CuO}_{4\pm\delta}$ . The component interval  $\Delta x$  is about 0.012. (b) The variation of  $c$ -axis lattice constant with increasing doping levels. In this figure,  $x$  refers to the nominal doping level. Reprinted by permission from Springer Nature Customer Service Centre GmbH: Springer Nature, Science China Physics, Mechanics and Astronomy, [54], 2017.

Initially, pinholes or slits made of anti-radiation materials were used to shrink the profile size of x-ray beams. Figure 12 shows the data collected from a combinatorial  $\text{La}_{2-x}\text{Ce}_x\text{CuO}_4$  library chip (an electron-doped copper oxide superconductor, where  $x$  varies from 0.10 to 0.19). A micro-area scan is realized by adding a narrow slot and a moving sample stage to a commercially available x-ray diffractometer [54]. The calculated  $c$ -axis lattice constant monotonically decreases while raising the nominal doping level  $x$ , in accordance with the tendency extracted from uniform LCCO thin films fabricated by conventional pulsed laser deposition (PLD) method [62, 63].

In this technique the analysis sensitivity and accuracy are unavoidably low, due to the limited incident x-ray throughput, which necessitates time-consuming and repetitive angular scanning measurements. To address this, techniques were developed using a zone plate as an x-ray focusing component or a 2D detector in order to enhance the intensity of the x-ray beam [64] or measurement efficiency [65]. In 2005, Luo *et al* developed a combinatorial x-ray analysis system with a spot size of 0.5 mm by using a polycapillary x-ray lens to focus the divergent beam from an x-ray source. This system, integrating micro-region x-ray diffraction, x-ray fluorescence, and x-ray photoluminescence tools, meets the requirements of high-throughput structure and composition characterizations. Instead of the angular dispersive x-ray diffraction, they used energy-dispersive x-ray diffraction (EDXRD), which uses the entire spectra of the focused x-ray, from 4 keV to 19 keV, without any moving parts. As a consequence, the measurement process was further accelerated. The configuration used in the system is shown in figure 13 [66]. More details about the operation principle of x-ray optics can be obtained, for example, in the review paper [67].

Concurrently, special x-ray sources were developed to meet the requirements of high-throughput characterizations. Xiang *et al* used a micro-beam x-ray system to simultaneously screen the composition and the structure with a resolution of 10–100  $\mu\text{m}$ . The x-ray intensity in such a system is 20 times higher than that of an ordinary x-ray source [32].

Since synchrotron facilities can offer high spatial resolution while simultaneously providing adequate photon flux, several high-throughput screening techniques were developed

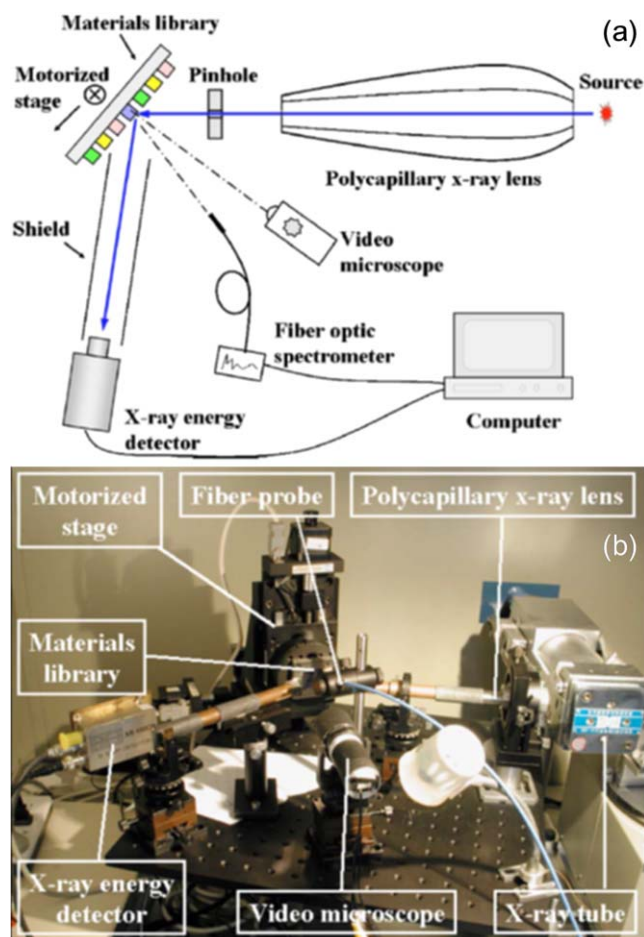


**Figure 13.** (a) Configuration and (b) photograph of the x-ray high-throughput characterization system. Reprinted from [66], with the permission of AIP Publishing.

specifically for such sources. In 1998, Isaacs *et al* used synchrotron x-ray micro-beam techniques to verify the feasibility of high-throughput characterization in combinatorial libraries [68]. This work included x-ray fluorescence, diffraction and absorption spectroscopy experiments with a spatial resolution of  $3 \times 20 \mu\text{m}^2$ . In 2014, combinatorial phase mapping techniques with a synchrotron source were realized by Gregoire *et al* [69]. The technique used in this work has the capability of measuring more than 5 000 samples per day, using synchrotron x-ray diffraction and fluorescence for rapid characterization. Xing *et al* recently improved the efficiency and automation even further [70]. The rate of recording diffraction images reached one pattern per second, and the diffraction patterns were automatically processed to create the composition phase map. In addition to commonly-used methods such as diffraction and fluorescence, x-ray absorption is also suitable for high-throughput characterization. For instance, Suram *et al* used a custom-made combinatorial x-ray absorption near-edge spectroscopy technique to obtain detailed chemical information on samples [71].

Although synchrotron x-ray facilities are powerful characterization tools, they remain a scarce resource, which impedes their use in high-throughput characterization. Developing more accessible rapid screening systems remains a major challenge in the field.

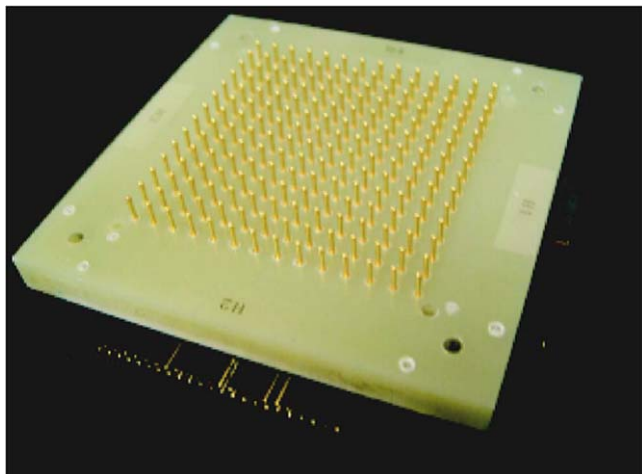


**Figure 14.** Image of the 196-pin device which makes electrical contact to the 49-sample thin film library for four-contact resistivity measurements. Reprinted from [72], with the permission of AIP Publishing.

### 3.2. Transport properties

Measuring transport properties such as resistivity, magnetoresistance and Hall effect is extremely important in uncovering the nature of superconductivity in various materials.

In 2005, Hewitt *et al* developed a 196-pin device to measure *dc* resistance versus temperature (shown in figure 14). The distance between nearest pins is about 4.64 mm. In the configuration of the van der Pauw method, these pins can establish 49 parallel channels in an epoxy plate of 4.2 inches  $\times$  4.2 inches. For low-temperature measurement, the device can be cooled to 7 K by cold fingers [72].

The sample chambers of most commercial low-temperature measurement systems, especially those equipped with magnets, have limited space. For high-throughput magnetoresistance measurements, a more compact probe, compatible with existing systems, is highly desirable. In 2013, Jin *et al* designed a high-throughput probe to search for superconductivity in the Fe-B composition spreads mentioned above. They used pogo pins for better contact between the sample surface and the pinpoint, and also shortened the distance between nearest pins to  $\sim 1$  mm. Thus, even if the lateral size of the sample chamber is limited to a centimeter scale, at least 16 multiplexed channels of temperature-dependent resistance can be measured at  $4 \times 4$  evenly spaced  $1 \text{ mm} \times 1 \text{ mm}$  areas in a van der Pauw configuration. Using this probe, the authors discovered superconductivity in the region where the ratio of Fe to B is approximately 1:2; there the superconducting transition temperature can reach 4 K. The temperature-dependent resistivity curves and a sketch diagram of the pogo pin array are shown in figure 2. A number of diced  $1 \text{ cm} \times 1 \text{ cm}$  chips from the superconducting region were measured using the 16-spot simultaneous resistance-versus-temperature measurement setup. Later, the device was upgraded and made compatible with a commercial physical property measurement system (PPMS). In this way, magnetoresistance and Hall data of a combinatorial film can be rapidly collected.

The Bozovic group performed multiple-channel measurements of the Hall signal and the resistivity by a

high-throughput system in order to characterize highly conductive oxides with Hall coefficients as small as  $10^{-10} \text{ m}^3/\text{C}$ . The receptacles of this device are shown in figure 15(a). There are 64 slots matching pogo pins (with a distance of 1.11 mm between adjacent pins), which contact the patterned film as shown in figure 15(b). In the center of the film, a stripe  $300 \mu\text{m}$  in width and 10 mm in length is bridged with 64 square pads covered with gold. The blocks for different channels segment the main stripe to  $300 \mu\text{m}$  in length. Using this device, 30 channels for the resistivity and 31 channels for the Hall resistivity can be measured simultaneously. Figure 15(c) shows a series of longitudinal resistivity  $\rho(T)$  curves from single  $\text{La}_{2-x}\text{Sr}_x\text{CuO}_4$ - $\text{La}_2\text{CuO}_4$  bilayer films. The doping resolution can reach  $\Delta x = 0.0002$  [73]. Due to the high special resolution of the Hall measurements, an intrinsic inhomogeneity of a sample could be detected. Wu *et al* were thereby able to construct a detailed phase diagram of this material and discovered a quantum charge cluster glass state that competes with the superconducting state [37].

Since in this design the current bridge is shared by all the channels, the sample should have good electrical conductivity. Thus, this pattern is not suitable for screening a combinatorial film with insulating areas. In such cases, an array micro-bridge design with independent current paths should be employed. In 2017, Wu *et al* reported a ‘sunbeam’ lithography pattern for simultaneous Hall measurements [74]. The 36 Hall bars, each with three pairs of transverse contacts (as sketched in figure 16(a)), form a circle with  $10^\circ$  between two successive bars. The angular dependence of  $\rho_T$  (transverse resistivity, defined as  $V_T d/I$ , where  $V_T$  is the voltage across the sample, transverse to the electrical current  $I$ , and  $d$  is the film thickness) and  $\rho$  in an under-doped ( $x = 0.04$ ) LSCO film shows  $\sin(2\varphi)$  oscillations; these suggest a breaking of the four-fold rotational symmetry of the crystal structure, as shown in figure 16(b). The fact that this anisotropy emerges in superconducting samples is significant, as its origin was attributed to electronic nematicity.

The spread of such methods is restricted by the difficulties of micro-fabrication. Shan *et al* took an alternative approach. They developed a scanning point contact probe compatible with PPMS. By mounting the sample on a moving stage consisting of close-loop z-axis and x-axis piezo cubes as shown in the left panel of figure 17, a Pt-Ir tip can be positioned on the sample surface with an accuracy of sub-micron scale. With this probe, He *et al* investigated the tunneling spectra of [111]-, [110]-, and [001]-oriented high quality  $\text{LiTi}_2\text{O}_4$  (LTO) thin films and unveiled anisotropic electron-phonon coupling in an LTO system [75]. The ability to probe local physical properties of superconductors will facilitate the rapid screening of superconducting combinatorial films without the need for complex micro-fabrication.

### 3.3. Magnetic properties

Since common probes with beams focused by optical lenses are commercially available, here we skip the description of magnetic-optical methods for high-throughput characterization. Scanning magnetic microscopes, e.g., the magnetic force microscope (MFM) [76–78], scanning Hall probe microscope

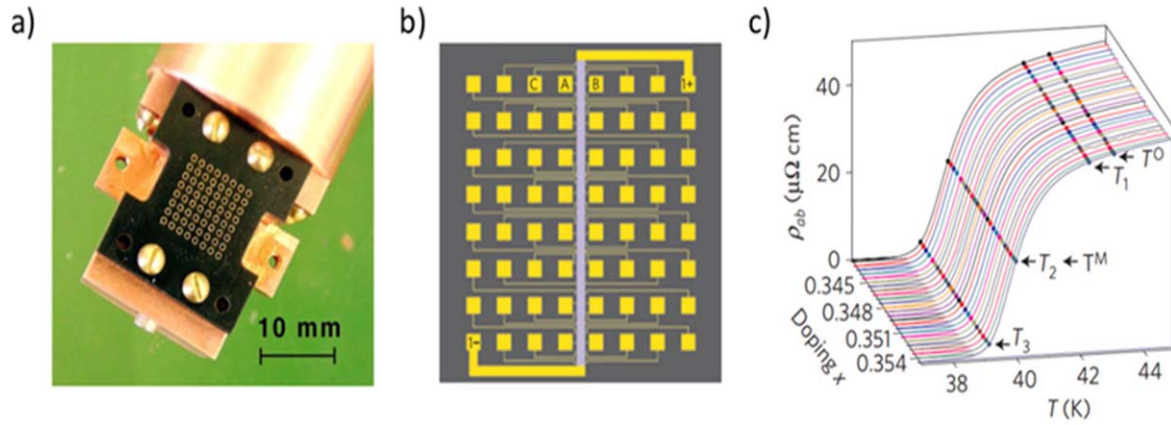


**Figure 15.** (a) Receptacles for spring-loaded pogo pins on the cryostat tail. (b) Film lithography and contact pattern. (c) The temperature-dependent *ab* plane resistivity  $\rho_{ab}$  measured from different channels on the same  $\text{La}_{2-x}\text{Sr}_x\text{CuO}_4\text{-La}_2\text{CuO}_4$  bilayer films. Reproduced with permission from [37]. PNAS April 19, 2016 113 (16) 4284-4289.

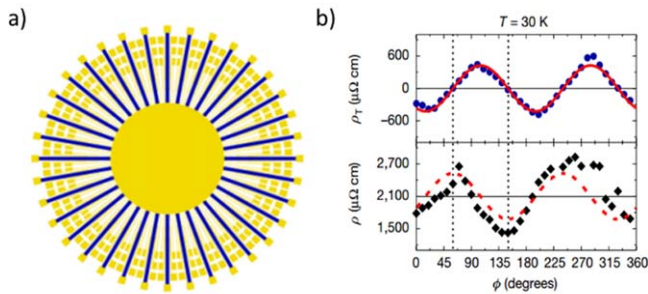


**Figure 16.** (a) The ‘sunbeam’ lithography pattern used for device fabrication contains 36 Hall bars, each with three pairs of transverse contacts. (b) The measured values of  $\rho_T(\varphi)$  and  $\rho(\varphi)$  at  $T = 30$  K. Reprinted by permission from Springer Nature Customer Service Centre GmbH: Nature 547 [74], 2017.

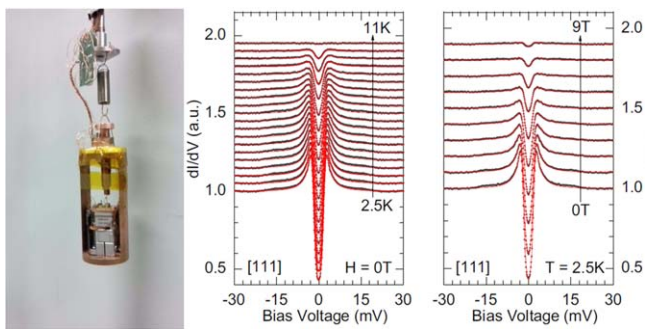


**Figure 17.** On the left: photograph of the scanning point contact probe. Middle and right panels: normalized differential conductance versus bias voltage for the [111] film, from 2.5 K to 10 K and from 0 to 9 T, respectively. Reprinted with permission from [75], Copyright (2017) by the American Physical Society.

(SHPM) [79, 80] and scanning superconducting quantum interference device (SQUID) [81–84], which possess the spatial resolution necessary for high-throughput magnetic imaging, have played and will continue to play an important role in understanding the nature of superconductivity.

The MFM, with a spatial resolution of about tens of nm, is generally based on measuring the force between a magnetized tip

and the scanned surface. This method shows potential for high-throughput mapping in both static and dynamic magnetic fields [85]. The MFM can study the topography of a sample and even image a single quantized vortex in a superconducting material [86]. The SHPM provides quantitative magnetic field measurements with a spatial resolution better than  $1 \mu\text{m}$  under general conditions. A sub-micron Hall probe can be manufactured and used to scan a sample with the aid of conventional scanning techniques [87]. Similar to the MFM, the SHPM can also image the distribution of quantized vortices in type-II superconductors [88]. Local magnetic fields can also be imaged by scanning with SQUIDs, which utilizes the effects of Cooper pair tunneling and superconducting quantum interference [89]. In contrast with the MFM and SHPM, scanning SQUIDs can obtain information about the local susceptibility and superfluid density, as shown in figure 18 [90]. Due to the lack of suitable combinatorial samples, these techniques are still rarely applied in high-throughput characterization of superconductors. However, their advantages and enormous potential cannot be ignored. Kogan and Kirtley have modeled the Meissner response of anisotropic superconductors and superconductors with inhomogeneous penetration depths [91, 92]. This makes it possible to extract the evolution of the penetration depth from a local diamagnetic susceptibility imaging of combinatorial superconducting films.

In addition to the transport and magnetic property characterization tools mentioned above, near-field detection techniques such as a scanning tip microwave near-field microscope (STMNM) were developed to probe the dynamic electromagnetic properties of superconductors.

Wei *et al* used a sharpened solid metal (instead of an aperture or a gap) as a point-like evanescent field emitter. Based on this design, they set up a near-field rf/microwave microscope that is capable of imaging surface resistance profiles with a spatial resolution of  $\sim 5 \mu\text{m}$  [93]. Later, Gao *et al* improved the spatial resolution to the order of 100 nm by introducing a sapphire disk with a center hole comparable to the diameter of the tip wire and a metal coating layer of  $1 \mu\text{m}$  on the surface, as shown in figure 19. In addition, a phase-sensitive technique was applied for faster data acquisition,

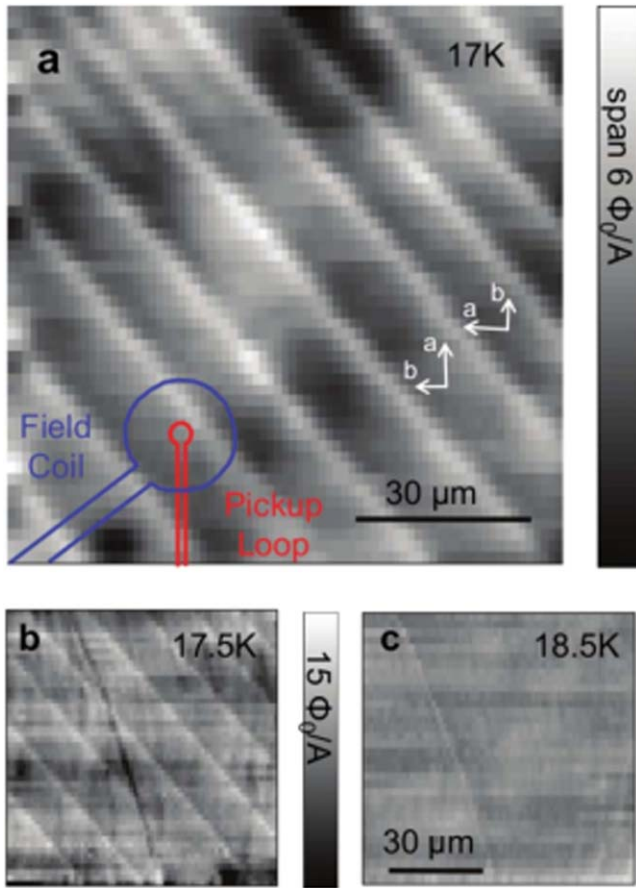


**Figure 18.** Local susceptibility image of the *ab* face of underdoped  $\text{Ba}(\text{Fe}_{1-x}\text{Co}_x)_2\text{As}_2$  with  $x = 0.051$  and  $T_c = 18.25$  K: (a) at  $T = 17$  K, sample, (b) at  $T = 17.5$  K, (c) at  $T = 18.5$  K. The brighter patterns indicate the regions with stronger diamagnetic responses, which disappear above  $T_c$ . Reprinted with permission from [90], Copyright (2010) by the American Physical Society.

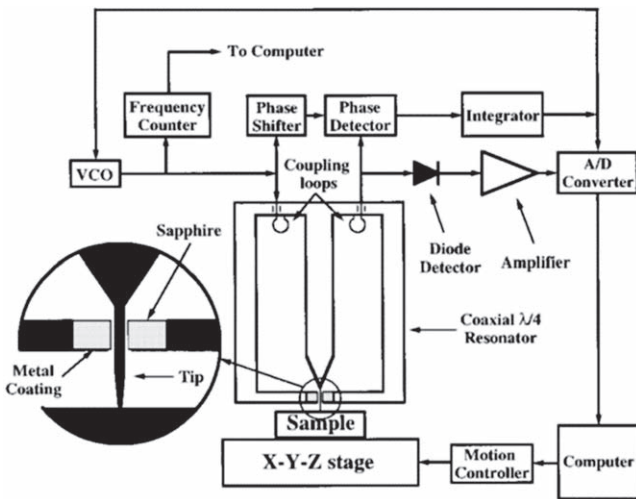


**Figure 19.** Schematic of the experimental setup for the STMNM with a resonator. Reprinted from [93], with the permission of AIP Publishing.

while a quasi-static theoretical model was developed to calculate the relative dielectric constant from the raw data [94].

In the same year, Takeuchi *et al* integrated the STMNM with a low-temperature cryostat and applied it to scan an

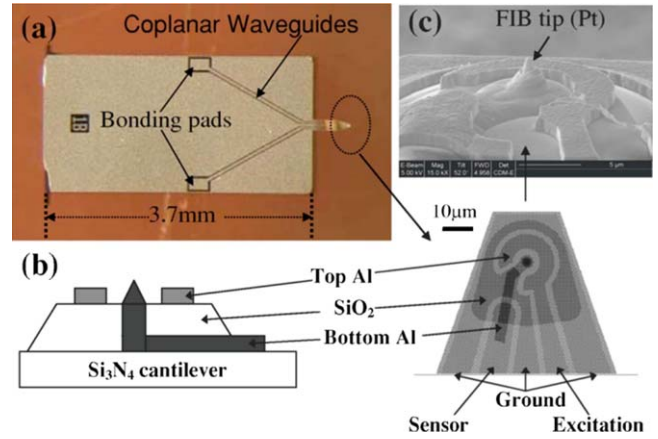


**Figure 20.** (a) Microfabricated cantilever with co-planar waveguides patterned on the top. The bonding pads and the chip dimension are labeled in the picture. (b) Schematics of the side view (left) and the top view (right) of the cantilever tip. All electrodes are labeled in the figure. (c) Scanning electron microscope (SEM) image of the Pt tip formed by focused ion beam (FIB) deposition. Reprinted from [96], with the permission of AIP Publishing.

$\text{YBa}_2\text{Cu}_3\text{O}_{7-\delta}$  film. The high-frequency response was used to detect the superconducting transitions at different positions on the film [95].

The Shen group designed a near-field scanning microwave microscope in a different manner. They separated the sensing probe from the excitation electrode to suppress the common-mode signal and used co-planar waveguides to transmit a microwave signal (shown in figure 20) [96]. Similarly, their microscope was later upgraded for low-temperature imaging [97].

In addition to composition, structure, electrical transport, and magnetism, methods were developed to image the thermal, optical, and mechanical properties of films [98–103]. From these measurements some key information about superconductivity can be obtained.

For example, Otani *et al* set up an integrated scanning spring probe system for high-throughput thermoelectric power-factor screening [101]. The schematic diagram can be seen in figure 21. Thermal transport measurements such as Nernst and thermopower are complementary to electrical transport results, and can be indispensable in clarifying issues related to multiband features [104], superconducting fluctuations [105] and phase transitions [106].

An imaging ellipsometer with a lateral resolution in the nanometer range was invented by Karageorgiev *et al*. As shown in figure 22, the system combines an ellipsometer with an atomic force microscope (AFM). The sample is illuminated from the bottom through a prism in total internal reflection (TIR), and the evanescent field created at the sample surface is scattered by a conventional AFM tip [107, 108]. The intensity of the measured optical signal depends on the sample thickness and local optical properties. By fitting the data and comparing with an existing database, the local thickness and other parameters such as the refractive index and absorption factor can be extracted [109, 110]. This can be extremely useful for studying interesting topics such as

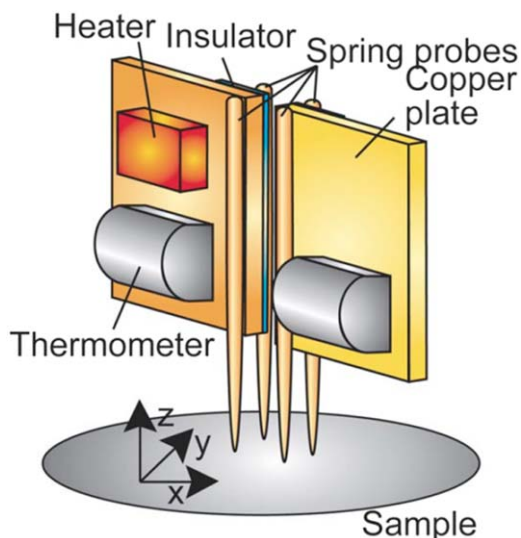


**Figure 21.** Schematic diagram of the probe to measure thermoelectric properties. Reprinted from [101], with the permission of AIP Publishing.

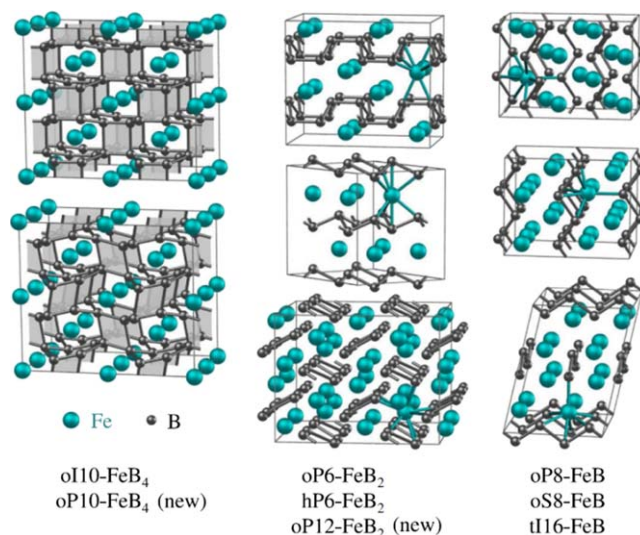


**Figure 23.** Competing B-rich Fe-B phases. Reprinted with permission from [134], Copyright (2010) by the American Physical Society.

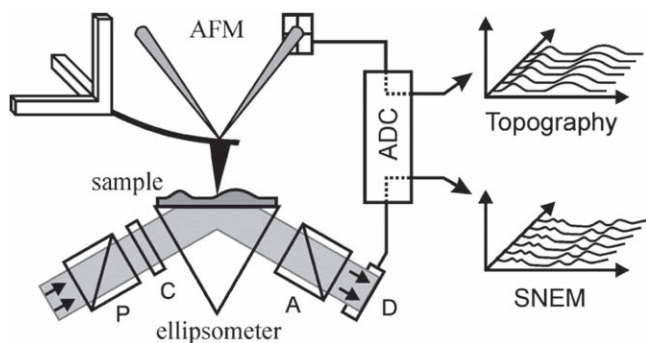


**Figure 22.** Experimental setup of scanning near-field ellipsometric microscope. Reprinted from [107], with the permission of AIP Publishing.

a possible negative index of refraction induced by surface Josephson-plasma waves in layered superconductors [111].

## 4. High-throughput theoretical calculations for superconductors

### 4.1. Introduction to high-throughput computations

In combinatorial materials studies, the range of possible combinations is so enormous that even high-throughput experiments can rarely or never cover it completely. So, in order to achieve an acceptable scale and rate of screening and optimizing, the number of candidate systems has to be restricted with the help of some heuristic or theoretical reasoning [112–115]. By using high-throughput calculations based on *ab initio* methods, molecular dynamics and Monte Carlo simulations, etc, a variety of properties for multiple materials can be predicted at a high rate, and can serve as starting points for subsequent

experiments. Furthermore, the combination of high-throughput computational results and experimental data can facilitate the construction of materials databases. These, in turn, can be mined and analyzed using materials informatics and artificial intelligence tools. Exploring the relations among the components, structure, and properties of materials can provide ideas for new materials designs.

High-throughput computations have already been employed in some research fields, such as solar water splitters [116, 117], solar photovoltaics [118], topological insulators [119], scintillators [120, 121], CO<sub>2</sub> capture materials [122], piezoelectrics [123], thermoelectrics [124, 125], hydrogen storage materials [126, 127], and Li-ion batteries [128–133].

### 4.2. High-throughput computations for superconductors

There have been several notable successful examples of discovery of superconductors with the help of high-throughput computations. Kolmogorov *et al* undertook an intensive study of the Fe-B system via *ab initio* high-throughput evolutionary calculations [134]. The crystal structure and formation energy for the entire Fe-B system was calculated, as shown in figure 23. Calculation of the electron-phonon coupling predicted *oP10-FeB<sub>4</sub>* to be a conventional superconductor. Stimulated by this theoretical study, high-throughput combinatorial research was subsequently devised and executed (details are given above) [36].

Matsumoto *et al* employed high-throughput computations to search for new thermoelectric or superconducting materials [135, 136]. By a data-driven materials search, they extracted from a database of inorganic materials (AtomWork) thousands of candidate materials with some specific characteristics (e.g., flat band). After further screening of the first-principles calculations, SnBi<sub>2</sub>Se<sub>4</sub> and PbBi<sub>2</sub>Te<sub>4</sub> were selected from all these candidates on the basis of their electronic structure (gap size, density of states near the Fermi level, etc). The authors

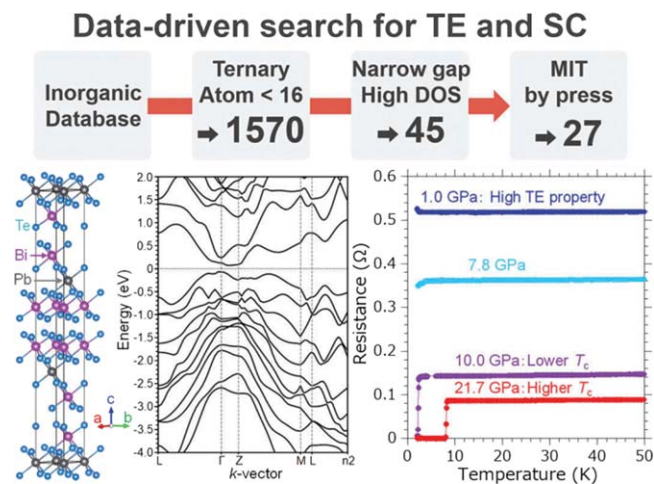


**Figure 24.** (a) Crystal structure, (b) band structure, (c) temperature dependence of resistance around superconducting transitions in  $\text{PbBi}_2\text{Te}_4$  under various pressures. Reproduced from [136]. CC BY 4.0.

successfully synthesized  $\text{SnBi}_2\text{Se}_4$  single crystal via a melt and slow cooling method (the exact composition is  $\text{SnBi}_{1.64}\text{Se}_{3.53}$ , as shown by energy dispersive x-ray spectroscopy). Superconducting transition was indeed observed under pressure. A sister compound,  $\text{PbBi}_2\text{Te}_4$ , also shows pressure-induced superconductivity, as shown in figure 24.

Other studies have applied *ab initio* high-throughput calculations on much larger scales. Klintonberg and Eriksson defined several distinct characteristics of the band structure of cuprates as key ingredients of their superconductivity [137]. They used these characteristics as criteria to filter through the calculated electronic structures of all materials in the Inorganic Crystallographic Structure Database (ICSD). Over 100 materials were identified as being potential HTSCs. A similar approach was used by Geilhufe *et al* with p-terphenyl, an organic material that shows signs of a superconducting transition at  $T_c \approx 123$  K when doped with potassium, used as a prototype [138]. A database containing the electronic structures of more than 10 000 organic crystals was searched, for compounds with similar densities of states (DOS). As a result, 15 materials were proposed as candidate HTSCs.

In the case of conventional superconductors, the mechanism of superconductivity is well understood, so their superconducting properties can be calculated from first principles, at least in theory. However, the specific mechanisms behind most examples of unconventional superconductivity are still not clear, and the electrons in these materials are often strongly correlated. Thus, attempts to predict new unconventional superconductors through deductive calculations are impossible, even in principle. Nevertheless, high-throughput computations can at least provide some rough guidance in the search for new superconductors.

High-throughput computations also speed up the construction of a database containing basic properties of new materials, which can be combined with machine learning methods to predict new superconductors (see next section), thus providing a new pathway for superconductivity research [138].

## 5. Machine learning for new superconductors

High throughput experiments often result in large data sets. Since it can be slow and impractical to analyse this data manually, the analysis step has become a common bottleneck for the entire process. Recent developments, however, permit a different approach to data analysis and, more generally, to the exploration of superconductors and the factors that determine the critical temperatures of various materials. Machine learning and statistical methods can use the information amassed in databases covering various measured and calculated materials properties in order to predict macroscopic variables, circumventing the need for theoretical models and complicated *ab initio* tools (for more details see, for example, Seko *et al* [139]).

The difficulties of modeling strongly correlated materials such as HTSCs provided an early impetus to the search for novel approaches. Application of statistical methods in the context of superconductivity began with simple clustering methods [140, 141]. These studies demonstrated that three ‘golden’ descriptors confine the 60 superconductors known at the time, with  $T_c > 10$  K to three small islands, while other superconductors are randomly dispersed in this space. Based on this observation, predictions for potential high-temperature superconductors were made. Another early work by Hirsch used statistical methods to look for correlations between normal state properties and the  $T_c$  of the metallic elements in the first six rows of the periodic table [142].

These studies were isolated early attempts to use data-driven approaches for the study of superconductivity. However, the recent significant increase of available data made possible the widespread use of machine learning algorithms to address a multitude of research questions. An investigation by Isayev *et al* in 2015 again found a clustering property of HTSC materials using structural and electronic properties data as predictors [143]. A classification model separating superconductors into two groups according to their  $T_c$  was developed and showed good performance. As a demonstration of the impact that machine learning can have in the search for superconductors, a sequential learning framework designed by Ling *et al* to discover the material with the highest  $T_c$  was evaluated on  $\sim 600$  known superconductors [144]. The framework performed significantly better than a method based on random guessing.

A work by Stanev *et al* in 2018 built upon many of the lessons from the earlier studies [38]. Whereas previous investigations explored several hundred compounds at most, this work considered more than 10 000 compositions. These were extracted from the SuperCon database, created and maintained by the National Institute for Materials Science in Japan. The database contains information such as  $T_c$  for an exhaustive list of all reported superconductors, as well as related non-superconducting compounds, including many closely-related materials varying only by small changes in stoichiometry. This unique information permitted the study of crucial subtleties in chemical composition among related compounds. The order-of-magnitude increase in training data

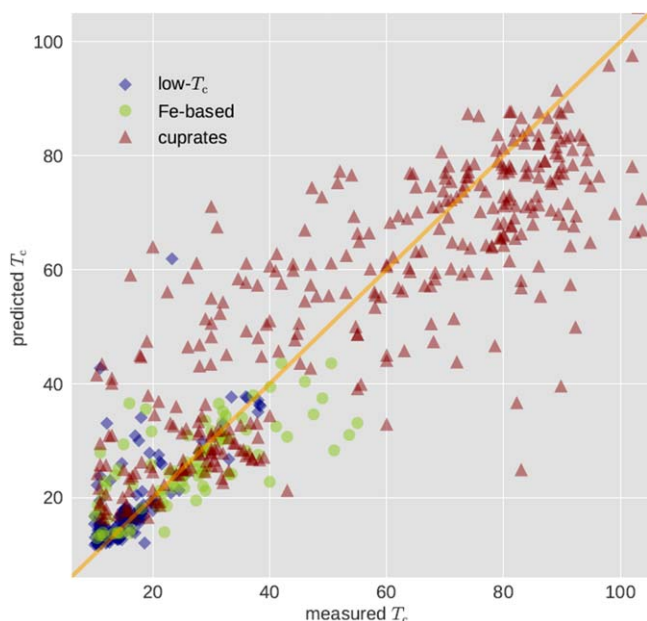


**Figure 25.** Performance of the regression model for  $T_c$  presented in [38]. Note the clear correlation between measured and predicted values. Reproduced from [38]. CC BY 4.0

also facilitated the optimizing and automation of the machine learning model construction procedures.

From SuperCon, a list of approximately 16 400 compounds was extracted, of which 4 000 have no  $T_c$  reported. Of these, roughly 5 700 compounds are cuprates and 1 500 are iron-based (about 35% and 9%, respectively), reflecting the significant research efforts invested in these two HTSC families.

To analyse the data, a classification model was developed, designed to separate materials into two distinct groups depending on whether  $T_c$  is above or below some pre-determined value. The temperature that separates the two groups,  $T_{\text{sep}}$ , was treated as an adjustable parameter of the model. For  $T_{\text{sep}} = 10$  K, the proportion of above- $T_{\text{sep}}$  materials is approximately 38%, while model accuracy is about 92%, i.e., the model can correctly classify nine materials out of ten, which is much better than random guessing.

Several regression models designed to predict the actual  $T_c$  values were presented, focused on materials with  $T_c > 10$  K (see figure 25). Separate models were constructed and trained on materials from cuprate and iron-based HTSC families, as well as with all other materials denoted ‘low- $T_c$ ’ for brevity. The differences in the used predictors across the family-specific models reflect the fact that distinct mechanisms are responsible for superconductivity in these groups.

Finally, the classification and regression models were integrated in a pipeline and employed for a high-throughput screening of the entire ICSD for candidate superconductors. First, a classification model was applied on this dataset to create a list of materials with a predicted  $T_c$  above 10 K. The list contained about 3 000 materials. The list was fed into a regression model trained on the entire SuperCon database to predict  $T_c$ . Filtering for the materials with  $T_c > 20$  K, the list

was reduced to about 2 000 compounds. The vast majority of the compounds identified as candidate superconductors were cuprate HTSC materials. There were also some materials clearly related to the iron-based superconductors. The remaining set has 35 members, and is composed of materials that are not obviously connected to any known superconducting family. The list can be divided into several distinct groups; especially interesting are the compounds containing heavy metals (such as Au, Ir, and Ru), metalloids (Se and Te), and heavier post-transition metals (Bi and Tl), which are or could be pushed into interesting, unstable oxidation states.

Although at the moment it is not clear whether any of the predicted compounds are superconducting, the presence of one highly unusual electronic structure feature in many of the candidates is encouraging: almost all of them exhibit one or several flat (or nearly flat) bands just below the energy of the highest occupied electronic state. Such bands lead to a large peak in the density of states and can cause a significant enhancement in  $T_c$ . Attempts to synthesize several of these compounds are underway.

In another very recent work, Xie *et al* used machine learning to obtain a closed-form approximation for  $T_c$  of phonon-driven superconductors, using an automatic algorithm to test a number of different functional forms [145]. The formula selected by the algorithm is more accurate than the commonly used approximation of McMillan, Allen and Dynes, demonstrating once again the great promise of machine learning in this field.

## 6. Conclusion and perspective

In this short review, some recent developments in superconductivity-related high-throughput techniques are summarized. Revealing the mechanisms of high-temperature superconductivity and discovering new and unconventional superconductors have always been important topics in condensed matter physics. As materials under study become more and more complex, the advantages of a high-throughput methodology become more pronounced. Although these advantages have proven to be significant, some limitations should also be pointed out. Currently, most high-throughput experiments are based on film techniques. This brings some specific constraints. Effects such as lattice mismatch and surface aging have to be considered. The number of possible combinations is limited, and the use of *in situ* measurements is often required. Moreover, in view of the reduced dimensions and surface reconstruction effects, the experimental results obtained from film samples may not reflect the intrinsic properties of bulk samples [146–149]. Such issues are present not only for superconductors, but for many other materials. In order to further accelerate the research on superconductors, as well as other functional materials, advances in the following three aspects are highly desirable.

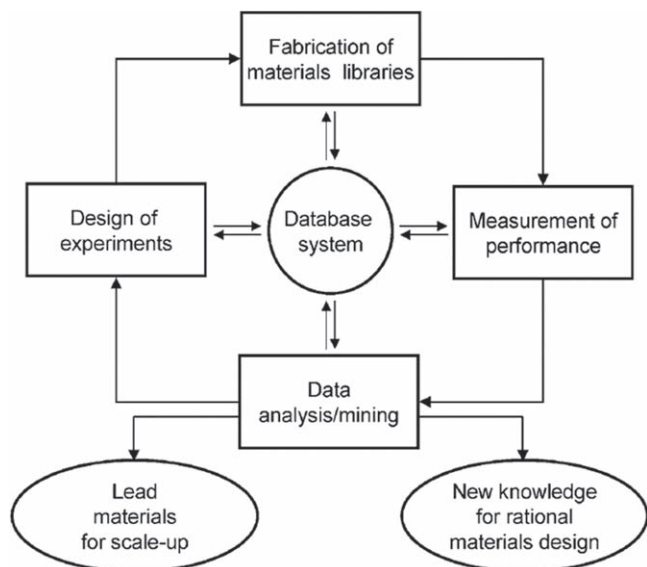


**Figure 26.** Typical combinatorial materials development cycle. Reprinted with permission from [154]. Copyright (2008) American Chemical Society.

### 6.1. New high-throughput techniques

While many combinatorial film preparation techniques have been developed, there is a great demand for high-precision characterization instruments, especially ones that can perform advanced spectroscopy measurements such as STM and angle resolved photoemission spectroscopy (ARPES). This requires combinatorial material libraries in the form of films to be measured *in situ*. Accordingly, combined systems such as combinatorial film STM and combinatorial film ARPES tools will be optimal. These will be especially beneficial for the study of superconducting combinatorial libraries. Characterization methods taking advantage of synchrotron sources should become widespread; these techniques allow the study of not only the composition and structure of materials, but also their elementary excitations. For instance, the resonant inelastic x-ray scattering (RIXS) technique can be used to measure spin excitation [150], charge excitation [151], phase of the order parameter [152], etc. Importantly, thin films can be probed with RIXS, since it requires only small sample volumes. Compared with the neutron scattering techniques, RIXS appears much more promising in high-throughput research on superconductivity [153].

### 6.2. Future high-throughput superconductivity research style

The high-throughput materials research paradigm is quite different from the traditional approaches, which can sometimes be compared to a ‘needle in a haystack’ search. Hanak proposed an integrated materials development workflow about 40 years ago [26]. Potyrailo and Mirsky extended the workflow by adding new elements, such as the planning of experiments and data mining, as shown in figure 26 [154].

Superconductivity research will certainly benefit from more widespread adoption of this paradigm, but it has its own specifics which should be taken into account. Currently, some characterization methods, such as STM, neutron scattering

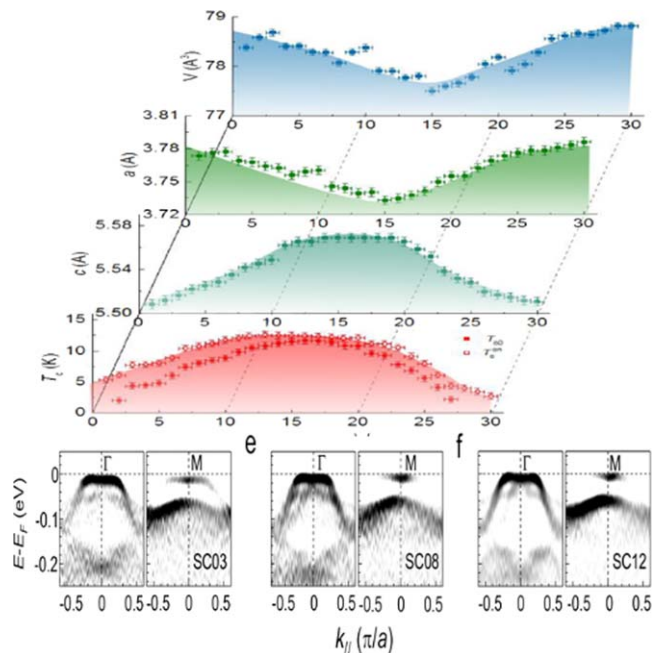


**Figure 27.** For FeSe film: the evolution of lattice constants from the  $T_c$  gradient combinatorial (upper panel); and the band structure of three uniform samples with different  $T_c$  values, obtained from ARPES (lower panel). Reproduced with permission from [57].

and ARPES, commonly used in the field, lag significantly behind the requirements of high-throughput screening. Thus, research on superconductivity, especially on mechanisms of high-temperature superconductivity, will have to combine studies of combinatorial libraries with exploration of conventional uniform films or bulk crystal samples. This was exemplified in the recent work on the relation between microstructure and  $T_c$  in FeSe superconductors. In this study the evolution of electrical transport properties and crystal lattice parameters were delineated by high-throughput experiments, whereas the electronic band structure was obtained from ARPES on uniform films (see figure 27) [57].

### 6.3. MGI platform

High-throughput methods, with their enormous potential to accelerate materials research, have already attracted significant attention. Some countries have started projects and programs in order to support the development of high-throughput computational tools. The U.S. Department of Energy created Scientific Discovery through Advanced Computing (SciDAC) in 2001 to develop new computational methods to tackle some of the most challenging scientific problems. In 2008, the U.S. National Academies created a new discipline, Integrated Computational Materials Engineering, which is the design of materials using a variety of software tools, either simultaneously or consecutively. In 2011 the U.S. launched the Materials Project, a core program of the Materials Genome Initiative (MGI), that uses high-throughput computing to uncover the properties of all known inorganic materials. The ‘Advanced Concepts in *ab initio* Simulations of Materials’ project, proposed by the European



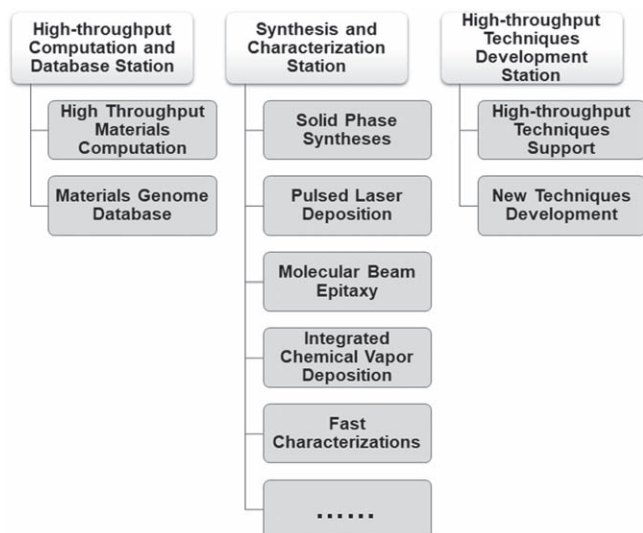


**Figure 28.** The organization of the Center for Materials Genome Initiative, Huairou, Beijing.

Science Foundation, aims to develop rapid *ab initio* calculations, which allow parameter-free calculations of real materials at the atomic level and are applicable to condensed matter systems.

However, in order to maximize the efficiency and impact of high-throughput methodology, it is necessary to closely coordinate the theoretical and experimental stages and combine computations with experiments and analyses of materials databases. One possible way of doing this is to integrate all the facilities on one big platform and organize them as nodes in an assembly line. The collected data can be standardized to establish a databank that can be shared. Techniques such as STM, neutron scattering and ARPES can contribute to the data collection, according to their limitations and characteristics. Since the MGI project was first announced in the U.S. in 2011 [155], several similar programs have been initiated in other countries. The Accelerated Metallurgy (AccMet) project initiated by the European Union, and the ‘MatNavi’ database managed by the National Institute for Materials Science in Japan, are programs established to develop novel materials research and development procedures. Among these programs, the Center for Materials Genome Initiative (CMGI) in Beijing, China may be the only one currently organized as a specialized high-throughput material research platform. This platform contains three large substations, as shown in figure 28: a high-throughput computation and database station, a high-throughput synthesis and fast characterization station, and a high-throughput technique research and development station. MGI and similar platforms have the potential to revolutionize materials research in the near future.

In conclusion, by integrating a novel research paradigm with new techniques, facilities, and platforms, high-throughput methodology is becoming more and more prominent in advancing the study of superconducting materials.

## Acknowledgments

The authors would like to thank M Y Qin, X Zhang, X Y Jiang, G He, Z P Feng, D Li, R Z Zhang, and J S Zhang for their help during preparation of the manuscript. This work was supported by the CAS Interdisciplinary Innovation Team, the Strategic Priority Research Program of the Chinese Academy of Sciences (XDB25000000), the National Key Basic Research Program of China (2015CB921000, 2016YFA0300301, 2017YFA0303003, and 2017YFA0302902), the National Natural Science Foundation of China (11927808, 11674374, 11804378 and 51672307), and the Key Research Program of Frontier Sciences, CAS (QYZDJ-SSW-SLH001 and QYZDB-SSW-SLH008). The work at the University of Maryland was supported by ONR (N000141512222 and N00014-13-1-0635), and AFOSR (FA 9550-14-10332).

## ORCID iDs

Kui Jin  <https://orcid.org/0000-0003-2208-8501>

## References

- [1] Bardeen J, Cooper L N and Schrieffer J R 1957 Microscopic theory of superconductivity *Phys. Rev.* **106** 162
- [2] Bardeen J, Cooper L N and Schrieffer J R 1957 Theory of Superconductivity *Phys. Rev.* **108** 1175
- [3] Ginzburg V L and Kirzhnits D A 1982 *High-Temperature Superconductivity* (New York: Springer US)
- [4] Flores-Livas J A, Boeri L, Sanna A, Profeta G, Arita R and Eremets M 2019 A perspective on conventional high-temperature superconductors at high pressure: methods and materials arXiv1905.06693 [*cond-mat.supr-con*]
- [5] Bednorz J G and Muller K A 1986 Possible high-Tc superconductivity in the Ba-La-Cu-O system *Z. Phys. B Con. Mat.* **64** 189–93
- [6] Adachi S, Takano S and Yamauchi H 1993 Superconductorization of GaSr<sub>2</sub>YCu<sub>2</sub>O<sub>7</sub> *J. Alloys Compd.* **195** 19–22
- [7] Korczak W, Perroux M and Strobel P 1992 Superconductivity in Sr<sub>0.85</sub>In<sub>0.15</sub>CuO<sub>2</sub>: extension to samarium *Physica C* **193** 303–8
- [8] Wu M K, Ashburn J R, Torng C J, Hor P H, Meng R L, Gao L, Huang Z J, Wang Y Q and Chu C W 1987 Superconductivity at 93 K in a new mixed-phase Y-Ba-Cu-O compound system at ambient pressure *Phys. Rev. Lett.* **58** 908–10
- [9] Zhao Z X *et al* 1987 Superconductivity above liquid-nitrogen temperature in Ba-Y-Cu oxides *Kexue Tongbao* **32** 661–4
- [10] Sun G F, Wong K W, Xu B R, Xin Y and Lu D F 1994 T<sub>c</sub> enhancement of HgBa<sub>2</sub>Ca<sub>2</sub>Cu<sub>3</sub>O<sub>8</sub> by Tl substitution *Phys. Lett. A* **192** 122–4
- [11] Kamihara Y, Watanabe T, Hirano M and Hosono H 2008 Iron-based layered superconductor La[O<sub>1-x</sub>F<sub>x</sub>]FeAs (x = 0.05–0.12) with T<sub>c</sub> = 26 K *J. Am. Chem. Soc.* **130** 3296–7
- [12] Hsu F C *et al* 2008 Superconductivity in the PbO-type structure alpha-FeSe *Proc. Natl. Acad. Sci. USA* **105** 14262–4
- [13] Wu W, Cheng J G, Matsubayashi K, Kong P P, Lin F K, Jin C Q, Wang N L, Uwatoko Y and Luo J L 2014 Superconductivity in the vicinity of antiferromagnetic order in CrAs *Nat. Commun.* **5** 5508

- [14] Chen R Y and Wang N L 2019 Progress in Cr- and Mn-based superconductors: a key issues review *Rep. Prog. Phys.* **82** 012503
- [15] Cheng J G and Luo J L 2017 Pressure-induced superconductivity in CrAs and MnP *J. Phys. Condens. Mat.* **29** 383003
- [16] Drozdov A P, Eremets M I, Troyan I A, Ksenofontov V and Shylin S I 2015 Conventional superconductivity at 203 kelvin at high pressures in the sulfur hydride system *Nature* **525** 73–6
- [17] Zhang L J, Wang Y C, Lv J and Ma Y M 2017 Materials discovery at high pressures *Nat. Rev. Mater.* **2** 17005
- [18] Wang Q Y *et al* 2012 Interface-induced high-temperature superconductivity in single unit-cell FeSe films on SrTiO<sub>3</sub> *Chinese Phys. Lett.* **29** 037402
- [19] Butko V Y, Logvenov G, Bozovic N, Radovic Z and Bozovic I 2009 Madelung strain in cuprate superconductors —a route to enhancement of the critical temperature *Adv. Mater.* **21** 3644–8
- [20] Ye J T, Zhang Y J, Akashi R, Bahramy M S, Arita R and Iwasa Y 2012 Superconducting dome in a gate-tuned band insulator *Science* **338** 1193–6
- [21] Lei B *et al* 2017 Tuning phase transitions in FeSe thin flakes by field-effect transistor with solid ion conductor as the gate dielectric *Phys. Rev. B* **95** 020503
- [22] Saadaoui H *et al* 2015 The phase diagram of electron-doped La<sub>2-x</sub>Ce<sub>x</sub>CuO<sub>4-δ</sub> *Nat. Commun.* **6** 6041
- [23] Zhang X, Yu H S, He G, Hu W, Yuan J, Zhu B Y and Jin K 2016 Transport anomalies and quantum criticality in electron-doped cuprate superconductors *Physica C* **525** 18–43
- [24] Mao S S 2013 High throughput growth and characterization of thin film materials *J. Cryst. Growth* **379** 123–30
- [25] Koinuma H and Takeuchi I 2004 Combinatorial solid-state chemistry of inorganic materials *Nat. Mater.* **3** 429–38
- [26] Hanak J J 1970 The ‘Multiple-Sample-Concept’ in materials research: synthesis, compositional analysis and testing of entire multicomponent systems *J. Mater. Sci.* **5** 964–71
- [27] Green M L, Takeuchi I and Hattrick-Simpers J R 2013 Applications of high throughput (combinatorial) methodologies to electronic, magnetic, optical, and energy-related materials *J. Appl. Phys.* **113** 231101
- [28] Iranmanesh M and Hulliger J 2016 Ceramic combinatorial syntheses exploring the chemical diversity of metal oxides *Prog. Solid State Chem.* **44** 123–30
- [29] Potyrailo R, Rajan K, Stoewe K, Takeuchi I, Chisholm B and Lam H 2011 Combinatorial and high-throughput screening of materials libraries: review of state of the art *ACS Comb. Sci.* **13** 579–633
- [30] Barber Z H and Blamire M G 2008 High throughput thin film materials science *Mater. Sci. Tech. – Lond.* **24** 757–70
- [31] Woo S I, Kim K W, Cho H Y, Oh K S, Jeon M K, Tarte N H, Kim T S and Mahmood A 2005 Current status of combinatorial and high-throughput methods for discovering new materials and catalysts *QSAR Comb. Sci.* **24** 138–54
- [32] Xiang X D 2004 High throughput synthesis and screening for functional materials *Appl. Surf. Sci.* **223** 54–61
- [33] Zhao J C 2006 Combinatorial approaches as effective tools in the study of phase diagrams and composition-structure-property relationships *Prog. Mater. Sci.* **51** 557–631
- [34] de Pablo J J *et al* 2019 New frontiers for the materials genome initiative *NPJ Comput. Mater.* **5** 41
- [35] Xiang X D, Sun X, Briceno G, Lou Y, Wang K A, Chang H, Wallace-Freedman W G, Chen S W and Schultz P G 1995 A combinatorial approach to materials discovery *Science* **268** 1738–40
- [36] Jin K, Suchoski R, Fackler S, Zhang Y, Pan X Q, Greene R L and Takeuchi I 2013 Combinatorial search of superconductivity in Fe-B composition spreads *APL Mater.* **1** 042101
- [37] Wu J, Bollinger A T, Sun Y and Bozovic I 2016 Hall effect in quantum critical charge-cluster glass *Proc. Natl. Acad. Sci. USA* **113** 4284–9
- [38] Stanev V, Oses C, Kusne A G, Rodriguez E, Paglione J, Curtarolo S and Takeuchi I 2018 Machine learning modeling of superconducting critical temperature *NPJ Comput. Mater.* **4** 29
- [39] Koinuma H, Aiyer H N and Matsumoto Y 2000 Combinatorial solid state materials science and technology *Sci. Technol. Adv. Mat.* **1** 1–10
- [40] Koinuma H 1998 Quantum functional oxides and combinatorial chemistry *Solid State Ionics* **108** 1–7
- [41] Kennedy K, Stefansk T, Davy G, Zackay V F and Parker E R 1965 Rapid method for determining ternary-alloy phase diagrams *J. Appl. Phys.* **36** 3808–10
- [42] Guerin S and Hayden B E 2006 Physical vapor deposition method for the high-throughput synthesis of solid-state material libraries *J. Comb. Chem.* **8** 66–73
- [43] Dahn J R, Trussler S, Hatchard T D, Bonakdarpour A, Mueller-Neuhaus J R, Hewitt K C and Fleischauer M 2002 Economical sputtering system to produce large-size composition-spread libraries having linear and orthogonal stoichiometry variations *Chem. Mater.* **14** 3519–23
- [44] Saadat M, George A E and Hewitt K C 2010 Densely mapping the phase diagram of cuprate superconductors using a spatial composition spread approach *Physica C* **470** S59–61
- [45] Xiang X D 1999 Combinatorial materials synthesis and high-throughput screening: an integrated materials chip approach to mapping phase diagrams and discovery and optimization of functional materials *Biotechnol. Bioeng.* **61** 227–41
- [46] Xiang X D 1999 Combinatorial materials synthesis and screening: an integrated materials chip approach to discovery and optimization of functional materials *Annu. Rev. Mater. Sci.* **29** 149–71
- [47] Xiang X D 1998 Combinatorial synthesis and high throughput evaluation of functional oxides—a integrated materials chip approach *Mat. Sci. Eng. B-Solid* **56** 246–50
- [48] Wang J and Evans J R G 2005 London University Search Instrument: a combinatorial robot for high-throughput methods in ceramic science *J. Comb. Chem.* **7** 665–72
- [49] Van Driessche I *et al* 2012 Chemical solution deposition using ink-jet printing for YBCO coated conductors *Supercond. Sci. Tech.* **25** 065017
- [50] Chen L, Bao J and Gao C 2004 Combinatorial synthesis of insoluble oxide library from ultrafine/nano particle suspension using a drop-on-demand inkjet delivery system *J. Comb. Chem.* **6** 699–702
- [51] Reddington E, Sapienza A, Gurau B, Viswanathan R, Sarangapani S, Smotkin E S and Mallouk T E 1998 Combinatorial electrochemistry: a highly parallel, optical screening method for discovery of better electrocatalysts *Science* **280** 1735–7
- [52] Yoo Y K and Xiang X D 2002 Combinatorial material preparation *J. Phys. Condens. Mat.* **14** R49–78
- [53] Fukumura T, Ohtani M, Kawasaki M, Okimoto Y, Kageyama T, Koida T, Hasegawa T, Tokura Y and Koinuma H 2000 Rapid construction of a phase diagram of doped Mott insulators with a composition-spread approach *Appl. Phys. Lett.* **77** 3426–8
- [54] Yu H S, Yuan J, Zhu B Y and Jin K 2017 Manipulating composition gradient in cuprate superconducting thin films *Sci. China Phys. Mech. Astron.* **60** 087421
- [55] McQueen T M *et al* 2009 Extreme sensitivity of superconductivity to stoichiometry in Fe<sub>1+δ</sub>Se *Phys. Rev. B* **79** 014522

- [56] Ohnishi T, Lippmaa M, Yamamoto T, Meguro S and Koinuma H 2005 Improved stoichiometry and misfit control in perovskite thin film formation at a critical fluence by pulsed laser deposition *Appl. Phys. Lett.* **87** 241919
- [57] Feng Z P *et al* 2018 High throughput research to elucidate tunable superconductivity in FeSe arXiv 1807.01273 [*cond-mat.supr-con*]
- [58] Wu J and Bozovic I 2015 Perspective: extremely fine tuning of doping enabled by combinatorial molecular-beam epitaxy *APL Mater.* **3** 062401
- [59] Koida T, Komiyama D, Koinuma H, Ohtani M, Lippmaa M and Kawasaki M 2002 Temperature-gradient epitaxy under *in situ* growth mode diagnostics by scanning reflection high-energy electron diffraction *Appl. Phys. Lett.* **80** 565–7
- [60] Feng Z P 2019 High-throughput investigation in superconducting films *University of Chinese Academy of Sciences* (China: Beijing)
- [61] Chikyow T, Ahmet P, Nakajima K, Koida T, Takakura M, Yoshimoto M and Koinuma H 2002 A combinatorial approach in oxide/semiconductor interface research for future electronic devices *Appl. Surf. Sci.* **189** 284–91
- [62] Naito M and Hepp M 2000 Superconducting  $T^*$ - $\text{La}_{2-x}\text{Ce}_x\text{CuO}_4$  films grown by molecular beam epitaxy *Jpn. J. Appl. Phys.* **2** **39** L485–7
- [63] Sawa A, Kawasaki M, Takagi H and Tokura Y 2002 Electron-doped superconductor  $\text{La}_{2-x}\text{Ce}_x\text{CuO}_4$ : preparation of thin films and modified doping range for superconductivity *Phys. Rev. B* **66** 014531
- [64] Rarback H *et al* 1988 Scanning x-ray microscope with 75 nm resolution *Rev. Sci. Instrum.* **59** 52–9
- [65] Ohtani M *et al* 2001 Concurrent x-ray diffractometer for high throughput structural diagnosis of epitaxial thin films *Appl. Phys. Lett.* **79** 3594–6
- [66] Luo Z, Geng B, Bao J, Liu C, Liu W, Gao C, Liu Z and Ding X 2005 High-throughput x-ray characterization system for combinatorial materials studies *Rev. Sci. Instrum.* **76** 095105
- [67] MacDonald C A 2017 Structured x-ray optics for laboratory-based materials analysis *Annu. Rev. Mater. Res.* **47** 115–34
- [68] Isaacs E D, Marcus M, Aeppli G, Xiang X D, Sun X D, Schultz P, Kao H K, Cargill G S and Haushalter R 1998 Synchrotron x-ray microbeam diagnostics of combinatorial synthesis *Appl. Phys. Lett.* **73** 1820–2
- [69] Gregoire J M, Van Campen D G, Miller C E, Jones R J, Suram S K and Mehta A 2014 High-throughput synchrotron x-ray diffraction for combinatorial phase mapping *J. Synchrotron Radiat.* **21** 1262–8
- [70] Xing H, Zhao B, Wang Y, Zhang X, Ren Y, Yan N, Gao T, Li J, Zhang L and Wang H 2018 Rapid construction of Fe-Co-Ni composition-phase map by combinatorial materials chip approach *ACS Comb. Sci.* **20** 127–31
- [71] Suram S K, Fackler S W, Zhou L, N'Diaye A T, Drisdell W S, Yano J and Gregoire J M 2018 Combinatorial discovery of lanthanum-tantalum oxynitride solar light absorbers with dilute nitrogen for solar fuel applications *ACS Comb. Sci.* **20** 26–34
- [72] Hewitt K C, Casey P A, Sanderson R J, White M A and Sun R 2005 High-throughput resistivity apparatus for thin-film combinatorial libraries *Rev. Sci. Instrum.* **76** 093906
- [73] Wu J, Pelleg O, Logvenov G, Bollinger A T, Sun Y J, Boebinger G S, Vanevic M, Radovic Z and Bozovic I 2013 Anomalous independence of interface superconductivity from carrier density *Nat. Mater.* **12** 877–81
- [74] Wu J, Bollinger A T, He X and Bozovic I 2017 Spontaneous breaking of rotational symmetry in copper oxide superconductors *Nature* **547** 432–5
- [75] He G *et al* 2017 Anisotropic electron-phonon coupling in the spinel oxide superconductor  $\text{LiTi}_2\text{O}_4$  *Phys. Rev. B* **95** 054510
- [76] Bruder C 1991 Magnetic force microscopy and superconductors *Physica C* **185** 1671–2
- [77] Reittu H J and Laiho R 1992 Magnetic force microscopy of Abrikosov vortices *Supercond. Sci. Technol.* **5** 448–52
- [78] Volodin A P and Marchevsky M V 1992 Magnetic force microscopy investigation of superconductors – 1st results *Ultramicroscopy* **42** 757–63
- [79] Chang A M, Hallen H D, Harriott L, Hess H F, Kao H L, Kwo J, Miller R E, Wolfe R, Vanderziel J and Chang T Y 1992 Scanning Hall probe microscopy *Appl. Phys. Lett.* **61** 1974–6
- [80] Chang A M, Hallen H D, Hess H F, Kao H L, Kwo J, Sudbo A and Chang T Y 1992 Scanning Hall-probe microscopy of a vortex and field fluctuations in  $\text{La}_{1.85}\text{Sr}_{0.15}\text{CuO}_4$  films *Europhys. Lett.* **20** 645–50
- [81] Matsumoto Y, Murakami M, Shono T, Hasegawa T, Fukumura T, Kawasaki M, Ahmet P, Chikyow T, Koshihara S and Koinuma H 2001 Room-temperature ferromagnetism in transparent transition metal-doped titanium dioxide *Science* **291** 854–6
- [82] Foley C P and Hilgenkamp H 2009 Why NanoSQUIDs are important: an introduction to the focus issue *Supercond. Sci. Tech.* **22** 064001
- [83] Bechstein S, Kohn C, Drung D, Storm J H, Kieler O, Morosh V and Schurig T 2017 Investigation of nanoSQUID designs for practical applications *Supercond. Sci. Tech.* **30** 034007
- [84] Persky E and Kalisky B 2018 Scanning SQUID view of oxide interfaces *Adv. Mater.* **30** 9
- [85] Martin Y and Wickramasinghe H K 1987 Magnetic imaging by force microscopy with 1000-Å resolution *Appl. Phys. Lett.* **50** 1455–7
- [86] Volodin A, Temst K, Bruynseraede Y, Van Haesendonck C, Montero M I, Schuller I K, Dam B, Huijbregtse J M and Griessen R 2002 Magnetic force microscopy of vortex pinning at grain boundaries in superconducting thin films *Physica C* **369** 165–70
- [87] Oral A, Bending S J and Henini M 1996 Real-time scanning Hall probe microscopy *Appl. Phys. Lett.* **69** 1324–6
- [88] Bluhm H, Sebastian S E, Guikema J W, Fisher I R and Moler K A 2006 Scanning Hall probe imaging of  $\text{ErNi}_2\text{B}_2\text{C}$  *Phys. Rev. B* **73** 014514
- [89] Koshnick N C, Huber M E, Bert J A, Hicks C W, Large J, Edwards H and Moler K A 2008 A terraced scanning superconducting quantum interference device susceptometer with submicron pickup loops *Appl. Phys. Lett.* **93** 243101
- [90] Kalisky B, Kirtley J R, Analytis J G, Chu J-H, Vaillonis A, Fisher I R and Moler K A 2010 Stripes of increased diamagnetic susceptibility in underdoped superconducting  $\text{Ba}(\text{Fe}_{1-x}\text{Co}_x)_2\text{As}_2$  single crystals: evidence for an enhanced superfluid density at twin boundaries *Phys. Rev. B* **81** 184513
- [91] Kogan V G 2003 Meissner response of anisotropic superconductors *Phys. Rev. B* **68** 104511
- [92] Kogan V G and Kirtley J R 2011 Meissner response of superconductors with inhomogeneous penetration depths *Phys. Rev. B* **83** 214521
- [93] Wei T, Xiang X D, WallaceFreedman W G and Schultz P G 1996 Scanning tip microwave near-field microscope *Appl. Phys. Lett.* **68** 3506–8
- [94] Gao C, Wei T, Duewer F, Lu Y L and Xiang X D 1997 High spatial resolution quantitative microwave impedance microscopy by a scanning tip microwave near-field microscope *Appl. Phys. Lett.* **71** 1872–4
- [95] Takeuchi I, Wei T, Duewer F, Yoo Y K, Xiang X D, Talyansky V, Pai S P, Chen G J and Venkatesan T 1997 Low temperature scanning-tip microwave near-field microscopy of  $\text{YBa}_2\text{Cu}_3\text{O}_{7-x}$  films *Appl. Phys. Lett.* **71** 2026–8

- [96] Lai K, Ji M B, Leindecker N, Kelly M A and Shen Z X 2007 Atomic force microscope-compatible near-field scanning microwave microscope with separated excitation and sensing probes *Rev. Sci. Instrum.* **78** 063702
- [97] Kundhikanjana W, Lai K J, Kelly M A and Shen Z X 2011 Cryogenic microwave imaging of metal-insulator transition in doped silicon *Rev. Sci. Instrum.* **82** 033705
- [98] Potyralo R A and Takeuchi I 2005 Role of high-throughput characterization tools in combinatorial materials science *Meas. Sci. Technol.* **16** 1–4
- [99] Oliver W C and Pharr G M 1992 An improved technique for determining hardness and elastic modulus using load and displacement sensing indentation experiments *J. Mater. Res.* **7** 1564–83
- [100] Wang J S, Yoo Y, Gao C, Takeuchi I, Sun X D, Chang H Y, Xiang X D and Schultz P G 1998 Identification of a blue photoluminescent composite material from a combinatorial library *Science* **279** 1712–4
- [101] Otani M, Lowhorn N D, Schenck P K, Wong-Ng W, Green M L, Itaka K and Koinuma H 2007 A high-throughput thermoelectric power-factor screening tool for rapid construction of thermoelectric property diagrams *Appl. Phys. Lett.* **91** 132102
- [102] Yan Y G, Martin J, Wong-Ng W, Green M and Tang X F 2013 A temperature dependent screening tool for high throughput thermoelectric characterization of combinatorial films *Rev. Sci. Instrum.* **84** 115110-7
- [103] Winkler G R and Winkler J R 2011 A light emitting diode based photoelectrochemical screener for distributed combinatorial materials discovery *Rev. Sci. Instrum.* **82** 114101
- [104] Jiang W, Mao S N, Xi X X, Jiang X G, Peng J L, Venkatesan T, Lobb C J and Greene R L 1994 Anomalous transport properties in superconducting  $\text{Nd}_{1.85}\text{Ce}_{0.15}\text{CuO}_{4\pm\delta}$  *Phys. Rev. Lett.* **73** 1291–4
- [105] Pourret A, Spathis P, Aubin H and Behnia K 2009 Nernst effect as a probe of superconducting fluctuations in disordered thin films *New J. Phys.* **11** 055071
- [106] Cyr-Choiniere O *et al* 2009 Enhancement of the Nernst effect by stripe order in a high- $T_c$  superconductor *Nature* **458** 743–5
- [107] Karageorgiev P, Orendi H, Stiller B and Brehmer L 2001 Scanning near-field ellipsometric microscope-imaging ellipsometry with a lateral resolution in nanometer range *Appl. Phys. Lett.* **79** 1730–2
- [108] Tranchida D, Diaz J, Schon P, Schonherr H and Vancso G J 2011 Scanning near-field ellipsometry microscopy: imaging nanomaterials with resolution below the diffraction limit *Nanoscale* **3** 233–9
- [109] Zhao M L, Lian J, Yu H S, Jin K, Xu L P, Hu Z G, Yang X L and Kang S S 2017 Dielectric functions of La-based cuprate superconductors for visible and near-infrared wavelengths *Appl. Surf. Sci.* **421** 611–6
- [110] Zhao M L, Lian J, Sun Z Z, Zhang W F, Li M M, Wang Y, Yu H S, Jin K and Hu X Y 2015 Ellipsometric study of the optical properties of n-type superconductor  $\text{La}_{1.9}\text{Ce}_{0.1}\text{CuO}_4$  *Opt. Mater. Express* **5** 2047–53
- [111] Golick V A, Kadygrob D V, Yampol'skii V A, Rakhmanov A L, Ivanov B A and Nori F 2010 Surface Josephson plasma waves in layered superconductors above the plasma frequency: evidence for a negative index of refraction *Phys. Rev. Lett.* **104** 187003
- [112] Gomez-Bombarelli R *et al* 2016 Design of efficient molecular organic light-emitting diodes by a high-throughput virtual screening and experimental approach *Nat. Mater.* **15** 1120–7
- [113] Chepul'skii R V and Curtarolo S 2009 First-principles solubilities of alkali and alkaline-earth metals in Mg-B alloys *Phys. Rev. B* **79** 134203
- [114] Jiang X and Zhao J J 2015 Evolution of boron clusters in iron tetraborides under high pressure: semiconducting and ferromagnetic superhard materials *RSC Adv.* **5** 48012–23
- [115] Landrum G A and Genin H 2002 The rational discovery Framework(TM): a novel tool for computationally guided high-throughput discovery *Mater. Res. Soc. Symp.* P **700** 233–8
- [116] Castelli I E, Landis D D, Thygesen K S, Dahl S, Chorkendorff I, Jaramillo T F and Jacobsen K W 2012 New cubic perovskites for one- and two-photon water splitting using the computational materials repository *Energ. Environ. Sci.* **5** 9034–43
- [117] Castelli I E, Olsen T, Datta S, Landis D D, Dahl S, Thygesen K S and Jacobsen K W 2012 Computational screening of perovskite metal oxides for optimal solar light capture *Energ. Environ. Sci.* **5** 5814–9
- [118] Yu L P and Zunger A 2012 Identification of potential photovoltaic absorbers based on first-principles spectroscopic screening of materials *Phys. Rev. Lett.* **108** 068701
- [119] Yang K S, Setyawan W, Wang S D, Nardelli M B and Curtarolo S 2012 A search model for topological insulators with high-throughput robustness descriptors *Nat. Mater.* **11** 614–9
- [120] Ortiz C, Eriksson O and Klintonberg M 2009 Data mining and accelerated electronic structure theory as a tool in the search for new functional materials *Comp. Mater. Sci.* **44** 1042–9
- [121] Setyawan W, Gaume R M, Lam S, Feigelson R S and Curtarolo S 2011 High-throughput combinatorial database of electronic band structures for inorganic scintillator materials *ACS Comb. Sci.* **13** 382–90
- [122] Lin L C *et al* 2012 *In silico* screening of carbon-capture materials *Nat. Mater.* **11** 633–41
- [123] Armiento R, Kozinsky B, Fornari M and Ceder G 2011 Screening for high-performance piezoelectrics using high-throughput density functional theory *Phys. Rev. B* **84** 014103
- [124] Curtarolo S *et al* 2012 A distributed materials properties repository from high-throughput *ab initio* calculations *Comp. Mater. Sci.* **58** 227–35
- [125] Wang S D, Wang Z, Setyawan W, Mingo N and Curtarolo S 2011 Assessing the thermoelectric properties of sintered compounds via high-throughput *ab initio* calculations *Phys. Rev. X* **1** 021012
- [126] Alapati S V, Johnson J K and Sholl D S 2006 Identification of destabilized metal hydrides for hydrogen storage using first principles calculations *J. Phys. Chem. B* **110** 8769–76
- [127] Lu J, Fang Z Z G, Choi Y J and Sohn H Y 2007 Potential of binary lithium magnesium nitride for hydrogen storage applications *J. Phys. Chem. C* **111** 12129–34
- [128] Chen H L, Hautier G, Jain A, Moore C, Kang B, Doe R, Wu L J, Zhu Y M, Tang Y Z and Ceder G 2012 Carbonophosphates: a new family of cathode materials for Li-ion batteries identified computationally *Chem. Mater.* **24** 2009–16
- [129] Kim J C, Moore C J, Kang B, Hautier G, Jain A and Ceder G 2011 Synthesis and electrochemical properties of monoclinic  $\text{LiMnBO}_3$  as a Li intercalation material *J. Electrochem. Soc.* **158** A309–15
- [130] Hautier G, Jain A, Chen H L, Moore C, Ong S P and Ceder G 2011 Novel mixed polyanions lithium-ion battery cathode materials predicted by high-throughput *ab initio* computations *J. Mater. Chem.* **21** 17147–53
- [131] Jain A, Hautier G, Moore C, Kang B, Lee J, Chen H L, Twu N and Ceder G 2012 A Computational Investigation of  $\text{Li}_9\text{M}_3(\text{P}_2\text{O}_7)_3(\text{PO}_4)_2$  ( $\text{M} = \text{V}, \text{Mo}$ ) as cathodes for Li ion batteries *J. Electrochem. Soc.* **159** A622–33
- [132] Chen H L, Hautier G and Ceder G 2012 Synthesis, computed stability, and crystal structure of a new family of inorganic

- compounds: carbonophosphates *J. Am. Chem. Soc.* **134** 19619–27
- [133] Wang X L, Xiao R J, Li H and Chen L Q 2017 Oxysulfide LiAlSO: a lithium superionic conductor from first principles *Phys. Rev. Lett.* **118** 6
- [134] Kolmogorov A N, Shah S, Margine E R, Bialon A F, Hammerschmidt T and Drautz R 2010 New superconducting and semiconducting Fe-B compounds predicted with an *ab initio* evolutionary search *Phys. Rev. Lett.* **105** 217003
- [135] Matsumoto R, Hou Z F, Hara H, Adachi S, Takeya H, Irifune T, Terakura K and Takano Y 2018 Two pressure-induced superconducting transitions in SnBi<sub>2</sub>Se<sub>4</sub> explored by data-driven materials search: new approach to developing novel functional materials including thermoelectric and superconducting materials *Appl. Phys. Express* **11** 093101
- [136] Matsumoto R *et al* 2018 Data-driven exploration of new pressure-induced superconductivity in PbBi<sub>2</sub>Te<sub>4</sub> *Sci. Technol. Adv. Mat.* **19** 909–16
- [137] Klintonberg M and Eriksson O 2013 Possible high-temperature superconductors predicted from electronic structure and data-filtering algorithms *Comp. Mater. Sci.* **67** 282–6
- [138] Geilhufe R M, Borysov S S, Kalpakchi D and Balatsky A V 2018 Towards novel organic high-T<sub>c</sub> superconductors: data mining using density of states similarity search *Phys. Rev. Mater.* **2** 024802
- [139] Seko A, Togo A, Tanaka I and Tanaka I 2018 *Descriptors for Machine Learning of Materials Data* (Nanoinformatics Singapore: Springer) ([https://doi.org/https://doi.org/10.1007/978-981-10-7617-6\\_1](https://doi.org/https://doi.org/10.1007/978-981-10-7617-6_1))
- [140] Rabe K M, Phillips J C, Villars P and Brown I D 1992 Global multinary structural chemistry of stable quasi-crystals, high-T<sub>c</sub> ferroelectrics, and high-T<sub>c</sub> superconductors *Phys. Rev. B* **45** 7650–76
- [141] Villars P and Phillips J C 1988 Quantum structural diagrams and high-T<sub>c</sub> superconductivity *Phys. Rev. B* **37** 2345–8
- [142] Hirsch J E 1997 Correlations between normal-state properties and superconductivity *Phys. Rev. B* **55** 9007–24
- [143] Isayev O, Fourches D, Muratov E N, Oses C, Rasch K, Tropsha A and Curtarolo S 2015 Materials cartography: representing and mining materials space using structural and electronic fingerprints *Chem. Mater.* **27** 735–43
- [144] Ling J, Hutchinson M, Antono E, Paradiso S and Meredig B 2017 High-dimensional materials and process optimization using data-driven experimental design with well-calibrated uncertainty estimates *Integr. Mater. Manuf. Innov.* **6** 207–17
- [145] Xie S R, Stewart G R, Hamlin J J, Hirschfeld P J and Hennig R G 2019 Functional form of the superconducting critical temperature from machine learning arXiv [1905.06780](https://arxiv.org/abs/1905.06780) [*cond-mat.supr-con*]
- [146] Douglass D H 1964 Superconducting thin films *Rev. Mod. Phys.* **36** 316
- [147] Ando T, Fowler A B and Stern F 1982 Electronic properties of two-dimensional systems *Rev. Mod. Phys.* **54** 437–672
- [148] Crittenden E C and Hoffman R W 1953 Thin films of ferromagnetic materials *Rev. Mod. Phys.* **25** 310–5
- [149] Dawber M, Rabe K M and Scott J F 2005 Physics of thin-film ferroelectric oxides *Rev. Mod. Phys.* **77** 1083–130
- [150] Minola M *et al* 2017 Crossover from collective to incoherent spin excitations in superconducting cuprates probed by detuned resonant inelastic x-ray scattering *Phys. Rev. Lett.* **119** 097001
- [151] Chen C C *et al* 2010 Unraveling the nature of charge excitations in La<sub>2</sub>CuO<sub>4</sub> with momentum-resolved Cu K-Edge resonant inelastic x-ray scattering *Phys. Rev. Lett.* **105** 177401
- [152] Marra P, Sykora S, Wohlfeld K and van den Brink J 2013 Resonant inelastic x-ray scattering as a probe of the phase and excitations of the order parameter of superconductors *Phys. Rev. Lett.* **110** 117005
- [153] Lin J Q *et al* 2019 Doping evolution of the charge excitations and electron correlations in electron-doped superconducting La<sub>2-x</sub>Ce<sub>x</sub>CuO<sub>4</sub> arXiv [1906.11354](https://arxiv.org/abs/1906.11354) [*cond-mat.supr-con*]
- [154] Potyrailo R A and Mirsky V M 2008 Combinatorial and high-throughput development of sensing materials: the first 10 years *Chem. Rev.* **108** 770–813
- [155] White A 2012 The materials genome initiative: one year on *MRS Bull.* **37** 715–6